



**HAL**  
open science

## **Periostin Promotes Cell Proliferation and Macrophage Polarization to Drive Repair after AKI**

Raphael Kormann, Panagiotis Kavvadas, Sandrine Placier, Sophie Vandermeersch, Aude Dorison, Jean-Claude Dussaule, Christos Chadjichristos, Niki Prakoura, Christos Chatziantoniou

► **To cite this version:**

Raphael Kormann, Panagiotis Kavvadas, Sandrine Placier, Sophie Vandermeersch, Aude Dorison, et al.. Periostin Promotes Cell Proliferation and Macrophage Polarization to Drive Repair after AKI. *Journal of the American Society of Nephrology*, 2020, 31 (1), pp.85-100. 10.1681/ASN.2019020113 . hal-02494252

**HAL Id: hal-02494252**

**<https://hal.sorbonne-universite.fr/hal-02494252>**

Submitted on 28 Feb 2020

**HAL** is a multi-disciplinary open access archive for the deposit and dissemination of scientific research documents, whether they are published or not. The documents may come from teaching and research institutions in France or abroad, or from public or private research centers.

L'archive ouverte pluridisciplinaire **HAL**, est destinée au dépôt et à la diffusion de documents scientifiques de niveau recherche, publiés ou non, émanant des établissements d'enseignement et de recherche français ou étrangers, des laboratoires publics ou privés.

**Periostin promotes cell proliferation and macrophage polarization to drive repair after acute kidney injury**

Raphaël Kormann<sup>1,2</sup>, Panagiotis Kavvadas<sup>1</sup>, Sandrine Placier<sup>1</sup>, Sophie Vandermeersch<sup>1</sup>, Aude Dorison<sup>1,2</sup>, Jean-Claude Dussaule<sup>1,2</sup>, Christos E. Chadjichristos<sup>1,2,\*</sup>, Niki Prakoura<sup>1,\*</sup> and Christos Chatziantoniou<sup>1,2,\*</sup>

<sup>1</sup>Institut National de la Santé Et de la Recherche Médicale UMRS 1155, Tenon Hospital, Paris, France; <sup>2</sup>Sorbonne Université, Paris, France.

\*CEC, NP and CC are co-last authors.

**Running title:** Periostin promotes repair in AKI

**Abstract word count:** 207

**Text word count:** 3,491

**Keywords:** Periostin, AKI, apoptosis, repair, macrophages

Correspondence:

Dr. Christos Chatziantoniou,

INSERM UMRS 1155,

Tenon Hospital, 4 rue de la Chine, 75020 Paris, France.

Email: [christos.chatziantoniou@upmc.fr](mailto:christos.chatziantoniou@upmc.fr)

Tel: (331) 56016653

Fax: (331) 56016659

## Significance Statement

AKI has been associated with increased morbidity and mortality or secondary organ dysfunctions. A better understanding of the mechanisms governing renal injury and repair may lead to a more efficient management of patients suffering from AKI. This paper identifies periostin, produced by damaged epithelial cells after murine ischemic injury, as a novel and important mediator of renal repair after AKI. It demonstrates that periostin protects epithelial cells from persistent cell cycle arrest and death and promotes a pro-regenerative macrophage phenotype, both of which contribute to a more efficient repair of the injured epithelium. Our findings provide novel insights in the repair mechanisms following AKI, which may contribute to a better care of AKI patients.

## Abstract

**Background:** Periostin, a matricellular protein, has been associated with progression of CKD in different animal models and patient specimens, but its role in AKI is still unknown.

**Methods:** To examine the role of periostin in AKI, we used mice with conditional tubule-specific periostin overexpression or global deletion in the renal ischemia/reperfusion (I/R) model, and primary tubular cell cultures in a model of hypoxia/re-oxygenation.

**Results:** Periostin was strongly produced by tubular epithelial cells at the repair phase of I/R. Periostin overexpression protected mice from I/R, while knock-out mice showed increased tubular injury and deteriorated renal function. Periostin interacted with its receptor integrin- $\beta$ 1 to inhibit tubular cell cycle arrest and apoptosis in both *in vivo* and *in vitro* models. The expression of proinflammatory molecules was diminished in periostin-overexpressing mice, with F4/80<sup>+</sup> macrophages being more abundant in overexpressing mice compared to knock-out mice after I/R. Macrophages from periostin-overexpressing mice showed increased

proliferation and expression of pro-regenerative factors after I/R, the opposite phenotype being observed in knock-out mice. Co-culture of hypoxia-treated primary tubules overexpressing periostin with a macrophage cell-line or recombinant periostin treatment directly induced macrophage proliferation and expression of pro-regenerative molecules.

**Conclusions:** Our results identify periostin as a novel and important mediator of the mechanisms controlling renal repair following AKI.

## **Introduction**

AKI is a dynamic process involving hemodynamic changes, inflammation, endothelial and epithelial cell damage, followed by repair and restoration of renal function. Ischemia/reperfusion (I/R) is among the primary causes of AKI.<sup>1</sup> The nature of the recovery response is dependent on the degree to which the injured cells can regenerate and restore normal function. A maladaptive response to AKI has been associated to secondary chronic kidney disease development.<sup>2</sup> AKI was also linked with distal organ effects, including pulmonary, cardiac, hepatic and neurologic dysfunction.<sup>3</sup> The mechanisms of injury and repair following AKI are not fully understood yet, with epithelial cells and macrophages being at the forefront of these processes.

Periostin is a 90 kDa secreted matricellular protein with high physiological expression in bone and dental tissues.<sup>4</sup> Although its expression in most adult tissues is low, periostin is *de novo* expressed during chronic disease of several organs, including the kidney, promoting inflammatory and fibrotic processes or proliferation.<sup>5-7</sup> Periostin exerts its functions by interacting with extracellular matrix components to drive collagen fibrillogenesis and remodeling<sup>8-10</sup> or by signaling through cell-surface integrin receptors to promote cell

adhesion, migration and proliferation.<sup>11-13</sup> Periostin is induced by different profibrotic factors like TGF- $\beta$ 1,<sup>4,10,14</sup> Angiotensin-II<sup>14</sup> and PDGF,<sup>15</sup> interleukins IL-4 and IL-13<sup>16,17</sup> or pro-inflammatory transcription factors like NF $\kappa$ B.<sup>18</sup> Although the association of periostin with CKD progression has been established in different experimental models and biopsy specimens,<sup>5,19</sup> the role of periostin in AKI is still unknown.

Here, we investigated the role of periostin in the model of I/R-induced AKI. Periostin was strongly *de novo* expressed by renal tubular cells at the repair phase of I/R. Mice lacking periostin showed worsened kidney structure and function, whereas mice conditionally overexpressing periostin in the renal tubules displayed highly preserved renal phenotypes both short-term and long-term after I/R. Subsequent studies revealed a direct effect of periostin in protecting epithelial cells from cell cycle arrest and death and promoting their proliferation. Moreover, periostin drove local macrophage proliferation after I/R and polarization to a pro-regenerative trophic phenotype. Our results describe for the first time a novel role for periostin as a protective factor in AKI, by regulating the fates of epithelial cells and macrophages to drive renal repair.

## **Methods**

### **Animals**

All procedures regarding animal experimentation were in accordance with the European Union Guidelines for the Care and Use of Laboratory Animals and approved by the local ethics committee of the National Institute for Health and Medical Research (INSERM). Animals were housed at constant temperature with free access to water and food.

The strain of periostin KO mice was created at the laboratory of Dr. Simon Conway and has been previously described.<sup>20</sup> The mice were used in the C57BL/6 background. WT littermates were used as controls.

Transgenic mice conditionally expressing periostin (POSTN) in tubular epithelial cells were created by crossing 3 different transgenic strains: (i) Pax8-rtTA (C57BL/6:DBA) mice expressing the reverse tetracycline-dependent transactivator (rtTA) under the control of the murine Pax8 promoter, (ii) LC1 mice (C57BL/6:BALB/c) where the expression of Cre recombinase is under control of the bidirectional  $P_{tet}$  promoter; when combined, they drive the expression of Cre recombinase in the renal tubular compartment after doxycycline administration. The two strains were kindly provided by Dr. Robert Koesters and have been previously described.<sup>21</sup> (iii) Tet-o-Periostin (FVB/N) mice which carry the mouse periostin cDNA downstream of a loxP-LacZ-loxP cassette under control of the  $P_{tet}$  promoter and were created at the genomic facilities of the Pitié Salpêtrière hospital in Paris. After extensive interbreeding, the genetic background of the transgenic mice was mixed consisting of FVB/N:C57BL/6:DBA:BALB/c. The primers and conditions used for genotyping of the transgenic mice are presented in Supplemental Table 1. Periostin expression was induced by administration of 0.2 mg/ml doxycycline in drinking water containing 2.5% sucrose for a period of 5 weeks starting 1 month after birth, after which the mice were subjected to ischemia/reperfusion. To examine the effect of periostin overexpression alone, doxycycline was administered to triple transgenic mice and double transgenic Pax8-rtTA/LC1-cre mice, serving as controls, for up to 4 months.

### **Ischemia/Reperfusion model**

8-10-week-old male KO mice and their WT littermates (n=7-8 per group) were anesthetized with intraperitoneal injection of ketamine (100 mg/kg)/xylazine (10 mg/kg) and subjected to right kidney nephrectomy. Right kidneys were used as controls (named CTL). The left renal artery was clamped for 30 minutes of warm ischemia at 37°C followed by 24 hours, 72 hours or 6 weeks of reperfusion. After reperfusion, the mice were euthanized, and blood and renal tissues were collected for subsequent analyses.

I/R on POSTN male mice, 9-10 weeks old (n=5-7) was performed as described above, after administration of doxycycline for 5 weeks. Double transgenic Pax8-rtTA/LC1-cre male mice of the same age treated with doxycycline for the same period were used as controls. After right nephrectomy, the left renal artery was clamped for 35 minutes followed by 24 hours, 72 hours or 6 weeks of reperfusion. The mice were euthanized, and blood and renal tissues were collected for subsequent analyses. This strain (FVB/N:C57BL/6:DBA:BALB/c mixed background) required increased clamping time compared to the KO strain (C57BL/6 background) because it is less sensitive to I/R injury.

### **Cell cycle analysis of TECs after I/R**

I/R 72h mice were sacrificed and the kidneys were collected, decapsulated and manually minced using a scalpel followed by dissociation in PBS, 0.5% BSA, 2mM EDTA in a GentleMACS Dissociator. The homogenate was filtered through a 30- $\mu$ m filter and centrifuged. The pellet was re-suspended in PBS/BSA/EDTA. The cells were fixed and permeabilized with the Foxp3/Transcription Factor Staining Buffer Set (ThermoFisher # 00-5523-00) and incubated with an anti-Pax8-FITC antibody (Biorbyt orb16164), followed by nuclear DNA staining with DAPI. An IgG-FITC isotype was used as control. The Pax8<sup>+</sup> tubular

cell population was selected, and the cell cycle phases were analyzed and quantified using MACSquant analyser 10 and Flowlogic software.

### **Primary culture of tubular epithelial cells (TECs)**

Primary tubular cells were isolated from periostin WT and KO mice or double transgenic Pax8-LC1 (CNT) and triple transgenic (POSTN) mice without prior doxycycline administration. The kidneys were manually minced and incubated with 1mg/ml collagenase I in PBS-0.5% BSA for 3 minutes at 37°C. 10% FBS-containing RPMI medium was added to de-activate the collagenase and the mixture was passed first through a 70-µm and then through a 40-µm filter (BD Falcon). The tubular epithelial cells were collected on the bottom of the 40-µm filter, seeded directly on culture plates in RPMI-10% FBS medium and cultured to confluence. For the immunofluorescence experiments, the cells were seeded on poly-L-lysine coated glass coverslips in culture plates.

### **Hypoxia treatment of cultured primary TECs**

To induce periostin overexpression prior to hypoxia, 80-90% confluent cultures of Pax8-LC1 (CNT) and triple transgenic (POSTN) primary tubular cells were treated with 1 µg/ml doxycycline in full medium for 2 days. To induce hypoxia, confluent cultures were incubated in 4 volumes of mineral oil on top of 1 volume of low-serum medium (RPMI-1% FBS) for 3h at 37°C, followed by extensive washing and reperfusion in full medium for 1-2h or 24h. Non-hypoxia treated cells were used as controls. After reperfusion, the cells were processed for protein extraction or immunofluorescence staining as described above. For the LDH assay, the cells were incubated with 75 µM or 125 µM of an Itgβ1 inhibitor (Anaspec, AS-62049) or a control RGD peptide (Anaspec, AS-62527) in RPMI-1% FBS medium for 2h prior to hypoxia.

### **H<sub>2</sub>O<sub>2</sub> treatment of cultured primary TECs**

Confluent cultures were incubated with 400  $\mu$ M H<sub>2</sub>O<sub>2</sub> in full medium to induce oxidative stress and apoptosis for 2h to 24h. The cells were processed for protein extraction or immunofluorescence staining, LDH or crystal violet assays as described below or in supplemental methods.

### **Renal macrophage isolation**

I/R 72h mice were sacrificed and the kidneys were collected, decapsulated and manually minced using a scalpel followed by dissociation in PBS, 0.5% BSA, 2mM EDTA in a MACS dissociator. The homogenate was filtered through a 30- $\mu$ m filter and centrifuged. The pellet was re-suspended in PBS/BSA/EDTA and incubated with anti-F4/80 magnetic microbeads (Miltenyi Biotec, 130-110-443) according to manufacturer's instructions. F4/80<sup>+</sup> cells were magnetically separated with LS columns and a MACS separator and then processed for RNA and protein extraction as described above. All equipment and antibodies were purchased from Miltenyi Biotec.

### **Co-culture of primary TECs with macrophages**

The murine macrophage RAW 264.7 cell line was purchased from Sigma and maintained according to manufacturer's instructions in 10% FBS-DMEM medium. Primary cultures of TECs, pretreated with doxycycline, were subjected to mineral-oil induced hypoxia as described above. RAW 264.7 macrophages were placed on top of TECs at re-oxygenation or normoxic TECs and co-cultures were maintained in low serum 1% FBS-DMEM medium for 48h. Co-cultures were then processed for RNA extraction, protein extraction or immunofluorescence as described previously.

### **Itgβ1 silencing of cultured primary TECs**

Transfection of cultured primary TECs with Itgβ1 siRNA or a negative control siRNA (TriFECTa DsiRNA Kit, mm.Ri.Itgb1.13, Integrated DNA Technologies) using HiPerFect transfection reagent (Qiagen) was performed according to manufacturer's instructions. Following transfection, the cells were treated with doxycycline for 48h to induce expression of periostin and were harvested for western blotting analysis or subjected to mineral-oil induced hypoxia followed by an LDH assay.

### **LDH assay**

The Cytotoxicity Detection Kit<sup>PLUS</sup> (LDH) from Roche (Cat. No. 04744926001) was used according to manufacturer's instructions. Confluent primary cultures transfected with Itgβ1 or a negative control siRNA and pretreated with doxycycline were subjected to mineral-oil induced hypoxia followed by 2h reperfusion, as described above. LDH release as an indicator of cell death was measured in culture medium using a spectrophotometer at 492 nm with a noise removal at 650 nm and normalized to the total LDH cell content. The results were expressed as percent LDH release.

### **Crystal violet viability assay**

After washing with PBS, cells were fixed in ethanol for 15 min and colored with crystal violet solution (Merck Millipore C.I.42555) for 20 minutes. Solubilization of the stain with 33% acetic acid was performed for an appropriate time (10-15 min), before measuring the absorbance at 590 nm in a spectrophotometer.

### **Treatment of RAW macrophages with recombinant periostin**

Sub-confluent cultures of RAW 264.7 cells were incubated overnight with low serum medium (1% FBS-DMEM) and treated with 1 µg/ml recombinant mouse periostin (rPostn, R&D Systems # 2955-F2-050) in 1% FBS-medium for 48h. Control cells were incubated with medium alone. The cells were collected for RNA extraction and quantitative real-time PCR or subjected to crystal violet assay for assessment of cell proliferation.

### **Statistical analysis**

Data are expressed as mean values +/- SEM. Analyses were performed using GraphPad Prism software. Data were analyzed using one-way ANOVA followed by a Fisher's test. Values of  $p < 0.05$  were considered significant.

### **Results**

#### **Periostin is strongly expressed at the repair phase of I/R by renal epithelial cells.**

Periostin gradually augmented from 24h (injury phase) to 72h (repair phase) after I/R in wild-type (WT) mice (Figure 1A-1B). Periostin was secreted and localized at the tubulointerstitial area after I/R, showing no expression in KO mice (Figure 1C). In situ hybridization showed that it was predominantly produced by renal tubular cells (Figure 1D). Co-localization of periostin with tubule-specific markers after I/R revealed that periostin was more abundant around injured proximal tubules and Henle loop, and less abundant around collecting ducts and distal tubular cells (Supplemental Figure 1).

To investigate the role of periostin in AKI, we performed I/R for 24h, 72h and 6weeks in two genetically modified strains; one conditionally overexpressing periostin by renal tubular cells (Pax8-rtTA system) (Figure 1E) and one lacking expression of periostin (periostin KO mice).

As controls for these strains, we used double transgenic Pax8-rtTA/LC1-cre (named CNT) or WT littermates, respectively. Periostin mRNA and protein expression was significantly augmented at the repair phase of I/R in control mice (CNT), while it was increased in periostin-overexpressing mice (POSTN) at all time points (Figure 1F). In both control and overexpressing mice, periostin was secreted at the tubulointerstitial area, while its expression pattern in control mice at 72h was similar to that of the overexpressing mice (Figure 1G).

### **Periostin protects from deterioration of renal structure and function after I/R.**

Periostin overexpression protected from severe tubular necrosis at 24h and 72h after I/R (Figure 2A-2C), while tubular dilation was also reduced (Figure 2D). Plasma creatinine and urea values were decreased in periostin-overexpressing mice at both time points, showing preserved renal function (Figure 2E-2F). The injury markers NGAL and KIM-1 and the expression of proinflammatory cytokines were attenuated in the overexpressing mice either at the injury phase (NGAL), the repair phase (MCP-1, VCAM-1) or at both time points after I/R (KIM-1, IL-6) (Figure 2G-2L).

In contrast, periostin KO mice showed increased tubular injury, plasma creatinine and urea at both 24h and 72h (Figure 3A-3D). The expression of KIM-1 and NGAL was augmented at 24h in periostin KO mice, indicating increased tubular damage (Figure 3E-3G). The kidney/body weight ratio was increased in both mouse strains after I/R independently of periostin expression (Supplemental Figure 2).

### **Periostin protects from cell cycle arrest and apoptosis and promotes proliferation after I/R.**

Since epithelial cell death and subsequent proliferation are major mechanisms of injury and repair in AKI, respectively, we examined the interaction of periostin with pathways of apoptosis and proliferation. Indeed, periostin-overexpressing mice displayed reduced expression of the cell-cycle arrest genes p21 and p16 both 24h and 72h after I/R (Figure 4A-4D). Activation of JNK, a kinase associated to cell stress and death, was prevented in periostin-overexpressing mice (Figure 4C-4D). Confirmatory, TUNEL (Figure 4E) and cleaved caspase-3 staining (Supplemental Figure 3A) were highly reduced in the overexpressing mice, indicating protection against apoptosis/cell death pathways. Cell cycle analysis of Pax8<sup>+</sup> tubular cells with flow cytometry 72h after I/R demonstrated decreased proportion of periostin-overexpressing tubular cells in G0G1 and increased proportion in S phase (Supplemental Figure 4A-4B).

TUNEL (Figure 4F) and cleaved caspase-3 staining (Supplemental Figure 3B) were increased in periostin KO mice after I/R, indicating increased apoptosis. Activation of AKT, a major pro-survival pathway, was higher in WT mice, while proteins associated to cell cycle arrest and death, like p53, p21 and BAX, were more highly induced in KO mice after I/R (Figure 4G-4H). A higher proportion of Pax8<sup>+</sup> tubular cells from KO mice was in the G0G1 phase after I/R compared to WT littermates, while a lower proportion was in the S and G2M cell cycle phases (Supplemental Figure 4C), indicating that periostin attenuates cell cycle arrest and promotes proliferation after I/R.

**Periostin inhibits hypoxia-induced epithelial cell death partially through interacting with Itgβ1.**

To investigate the mechanisms of periostin-mediated protection after AKI, we examined the expression of potential periostin receptors. Itgβ1 gradually augmented on the basal side of tubular epithelial cells from 24h to 72h after I/R (Figure 5A), with no major expression differences between groups (Figure 5B-5C). Co-immunoprecipitation with an Itgβ1 antibody revealed that periostin specifically interacted with integrin beta-1 after I/R (Figure 5D). Itgβ1 downstream targets FAK and ERK were more highly activated in KO mice, and p-ERK was less increased in periostin-overexpressing mice at 24h (Supplemental Figure 5). This suggests that periostin-Itgβ1 interaction leads to lower Itgβ1-associated signaling after I/R, which may be linked to periostin-mediated protection.

We studied the direct effects of periostin in primary cultures of isolated tubular cells subjected to mineral oil-induced hypoxia. Although Itgβ1 expression did not change after re-oxygenation, periostin gradually increased from 1h to 24h of re-oxygenation after hypoxia, mimicking its expression pattern in the mouse model (Figure 6A). Immunofluorescence studies showed that the epithelial layer lost its integrity and the interaction pattern mediated by Itgβ1 after hypoxia, this phenotype being markedly ameliorated in cells overexpressing periostin (Figure 6B). Periostin-overexpressing cells showed decreased apoptosis (Figure 6C) and a blunted induction of cell cycle arrest and pro-apoptotic proteins after hypoxia, including p53, p21, p-CDK1 and p-JNK (Figure 6D-6E). Periostin-overexpressing cells displayed lower LDH release and death compared to control cells after hypoxia, while Itgβ1 silencing increased the LDH release of both strains indicating that both Itgβ1 and periostin are implicated in cell survival after hypoxia (Figure 6F-6G).

Moreover, H<sub>2</sub>O<sub>2</sub>-induced oxidative stress increased the death of primary periostin KO tubular cells compared to WT, reflected by the increased caspase-3 activation and LDH release, and the decreased cell survival of KO cells (Supplemental Figure 6A-6C). Periostin was produced

by WT tubular cells and it was absent in KO cells, while Itgβ1 was similarly expressed in both cell types. As in the mouse model, AKT activation was higher in periostin-expressing cells, while p53 was more increased in KO cells after H<sub>2</sub>O<sub>2</sub> (Supplemental Figure 6D).

**Periostin induces local proliferation of macrophages in the kidney and polarization to a pro-regenerative phenotype.**

F4/80<sup>+</sup> macrophages were more abundant in periostin-overexpressing mice at the repair phase of I/R (Figure 7A). This increase was associated with higher proliferation of F4/80<sup>+</sup> macrophages in the overexpressing mice, assessed by co-staining with the proliferation markers MCM2 and PCNA (Figure 7B-7C). Respectively in periostin KO mice, F4/80<sup>+</sup> macrophages were less abundant and showed lower proliferation compared to WT mice (Figure 7D-7F).

F4/80<sup>+</sup> macrophages isolated from periostin-overexpressing mice showed decreased expression of IL-6, a proinflammatory cytokine linked to damage caused by I/R, and increased expression of macrophage genes/markers associated to M2c polarization and cell regeneration, like CD163, IL-10, CSF-1, uPA and LIF (Figure 8A). The increased expression of CD163, uPA and LIF was further confirmed at the protein level (Figure 8B). Consistently, periostin KO mice showed decreased abundance of CD206<sup>+</sup> macrophages and lower macrophage expression of IL-10 (Figure 8C-8D), indicating decreased M2 polarization.

Subsequently, we co-cultured primary tubular cells from control and overexpressing mice after being submitted to hypoxia, with a macrophage cell line (RAW 264.7). Our results showed inhibition of IL-6 and a bigger induction of HB-EGF, uPA and LIF (Figure 8E-8F), as well as cell proliferation (Figure 8G) in macrophages co-cultured with periostin-overexpressing cells. Moreover, treatment of RAW macrophages with recombinant periostin

(rPostn) directly inhibited the expression of IL-6 and IL-1 $\beta$ , and induced the expression of IL-10, CD163, uPA and LIF, as well as the cell proliferation (Supplemental Figure 7).

### **Periostin does not induce chronic fibrosis development either alone or after I/R.**

To examine whether periostin overexpression could induce spontaneous fibrosis development, we administered doxycycline to the transgenic mice for up to 4 months. Collagen 1 and collagen 3 expression as well as interstitial Sirius Red staining were similar in control and periostin-overexpressing mice up to 4 months of doxycycline administration, despite high periostin levels in the overexpressing mice (Supplemental Figure 8A-8E). Moreover, although the expression of profibrotic genes was increased at the repair phase of I/R, it was less induced in periostin-overexpressing mice (Supplemental Figure 8F-8H). This effect was maintained up to 6 weeks after I/R, since periostin-overexpressing mice displayed less Sirius Red and collagen I staining, with KO mice showing more interstitial fibrosis and collagen I accumulation, compared to their respective controls (Supplemental Figure 9A-9D). Of note, periostin levels were lower 6 weeks after I/R (Supplemental Figure 9E-9F), compared to the increase observed at the repair phase in both strains (Figure 1).

### **Discussion**

The major finding of this study is that periostin plays a protective role following I/R-induced AKI, thus contrasting its detrimental role during CKD. Using two different transgenic strains, mice conditionally overexpressing periostin in the renal epithelium and mice lacking periostin, we showed for the first time that periostin prevents renal epithelial damage after I/R by at least two mechanisms: protecting epithelial cells from cell cycle arrest and death and promoting a pro-regenerative macrophage phenotype, thus favoring epithelial repair.

The successful regeneration of the injured epithelium and the switching of macrophages to a pro-reparative phenotype are believed to play a major role in the response to AKI.

Periostin was *de novo* expressed and secreted by damaged epithelial cells after I/R. Periostin protected from early tubular damage and aggravation of renal function by inhibiting epithelial cell death 24h after I/R. This was demonstrated by the increased levels of pro-apoptotic proteins (p53, p21, BAX) and TUNEL staining in KO mice. Deletion of p53 or BAX in tubular epithelial cells inhibits renal damage and apoptosis after I/R.<sup>22,23</sup> Activation of AKT, a pro-survival kinase, was increased in WT mice, potentially limiting pro-apoptotic signals. Periostin was shown to directly activate AKT in several diseases and contexts.<sup>24-26</sup> p21 is strongly induced by p53 in epithelial cells after AKI.<sup>22,27</sup> p21 and p16 contribute to growth arrest and stress-induced premature senescence, leading to JNK activation, proliferative arrest and apoptosis.<sup>28,29</sup> However, the consequences of tubular growth arrest or proliferation in AKI were shown to be time- and context-dependent. Early proliferation of heavily damaged cells may promote further damage, therefore initial cell cycle blockade, e.g. through ischemic preconditioning<sup>30</sup> or CDK4/6 inhibition<sup>31</sup> before I/R led to ameliorated kidney injury. Later in the course of AKI or in case of less damaged cells, cell cycle activation is beneficial. Periostin diminished the induction of p21 and p-JNK after I/R and inhibited a late increase of both p21 and p16 in overexpressing mice, enabling cell cycle progression.

Renewal of the injured tubular epithelium is believed to be the predominant mechanism of repair after ischemic AKI.<sup>32</sup> De-repression of cell cycling by periostin was associated with induction of reparative proliferation 72h after I/R. Lack of periostin resulted in higher G0G1 proportion and reduced S and G2M phase abundance of tubular cells, while periostin

overexpression led to decreased tubular G0G1 and increased S phase abundance at the repair phase of I/R. Integrins allow cells to sense and respond to microenvironmental signals, being crucial for the adhesion, survival, proliferation and differentiation of most cell types.<sup>33</sup> Itgβ1 controls proliferation and cell cycle regulation, its conditional deletion leading to defective growth of different epithelial cell types.<sup>33</sup> In a recent study, Itgβ1 was essential in maintaining skeletal muscle cell homeostasis, regeneration and growth after experimentally induced muscle injury or in aged and dystrophic muscles through activation of ERK and AKT pathways.<sup>34</sup> In I/R-induced AKI, Itgβ1 was increased in tubular cells towards the repair phase and directly interacted with periostin. Except for increased AKT activation in WT mice, other Itgβ1 signaling targets like FAK and ERK were more highly activated in KO mice after I/R. This may suggest that periostin-Itgβ1 interaction differentially affects Itgβ1 signaling, and/or that increased FAK and ERK activation reflect higher tubular damage. In a model of mineral oil-induced hypoxia of cultured primary tubular cells, periostin was strongly induced at the late phase of re-oxygenation after hypoxia, consistent with the I/R model. Cells overexpressing periostin maintained the epithelial layer integrity and showed lower activation of pro-apoptotic and cell cycle arrest pathways, evidenced by the reduced TUNEL and p-JNK levels, as well as the decreased expression of p53, p21 and p-CDK1.<sup>35-37</sup> Consistently, H<sub>2</sub>O<sub>2</sub>-induced oxidative stress increased the expression of p53 in primary cultures of periostin KO tubular cells, which was associated with a lack of p-AKT signaling. Itgβ1 silencing in vitro before hypoxia increased further the LDH release and death of periostin-overexpressing cells, indicating that both Itgβ1 and periostin are implicated in cell survival after injury. On the other hand, recombinant periostin was shown to augment the death and expression of fibrotic proteins in cultured tubular cells after 24h of hypoxia.<sup>38</sup> These results are not contradictory to those presented here, since the authors performed a longer hypoxia

treatment without re-oxygenation which reflects long-term injury conditions associated with CKD.

The reparative capacity of the injured epithelium is influenced by local immune responses to tissue damage, with macrophages being a central coordinator of tissue injury and repair.<sup>39</sup> Upon injury, resident macrophages are supplemented by actively recruited infiltrating monocytes which differentiate into a proinflammatory pool known as M1 or classically activated macrophages. Macrophages respond to a combination of factors which drives their transition to the M2a or alternatively activated phenotype to coordinate tissue repair.<sup>40,41</sup> Several mechanisms contribute to their deactivation and priming towards an anti-inflammatory and pro-regenerative phenotype, namely M2c, displaying immunosuppressive effects.<sup>40,41</sup> The switch from the M1 to the M2 phenotype manifests the transition from the injury to the repair phase in the ischemically injured kidney and is necessary for tubular cell proliferation and functional recovery.<sup>42</sup>

Our results indicate that epithelial cell-derived periostin promotes a M2 macrophage phenotype assisting in tubular repair. Renal macrophages from WT mice displayed increased levels of M2 markers like mannose receptor (CD206) and IL-10 at the repair phase of I/R compared to those of KO mice. This tendency towards an M2 phenotype was associated with a higher intra-renal macrophage proliferation in WT mice. In glioblastoma xenografts, periostin secreted by stem cells was shown to promote the tumor recruitment of macrophages and their polarization to an M2 phenotype.<sup>43</sup>

Accordingly, periostin-overexpressing mice displayed a more abundant macrophage population at the repair phase of I/R, which was attributed to increased local macrophage proliferation compared to the control mice. Recently, it was shown that resident macrophages can directly proliferate in tissue without requirement for blood monocyte recruitment in the context of Th2-mediated inflammation.<sup>44,45</sup> Macrophages isolated from periostin-overexpressing mice displayed a less proinflammatory and a more pro-regenerative phenotype, showing increased expression of M2c markers like CD163 and IL-10 and higher production of pro-regenerative factors like CSF-1, LIF and uPA. Inhibition of CSF-1 was associated with decreased numbers of renal macrophages and impaired recovery after AKI,<sup>46</sup> while LIF and uPA were linked to a M2c macrophage phenotype promoting regeneration after muscle injury.<sup>47</sup> LIF was also associated with tubular regeneration after renal I/R in rats.<sup>48</sup> M2a markers Arg1 and Ym1 were downregulated in isolated macrophages of periostin-overexpressing mice (Supplemental Figure 10). This could be attributed to the fact that periostin overexpression protected from early tubular injury, limiting the requirement for pro-reparative M2a macrophages. Co-culture of macrophages with primary tubular cells from periostin-overexpressing mice subjected to hypoxia induced a higher expression of pro-regenerative factors and an increased proliferation of macrophages than co-culture with control cells. Moreover, treatment of macrophages with exogenous periostin had a similar effect, indicating that periostin directly promotes macrophage proliferation and polarization. Periostin secreted by cancer stem cells was shown to recruit macrophages through direct interaction with its receptor  $\alpha v\beta 3$ , followed by receptor associated AKT activation.<sup>43</sup>

In contrast to the previously established detrimental role of periostin in CKD, we unexpectedly discovered a protective role of periostin in AKI. Previous studies in various

animal models of CKD<sup>5,6,15,18,20</sup> and chronic diseases of other organs<sup>5-7</sup> showed that periostin promotes maladaptive epithelial proliferation, inflammatory cell infiltration and matrix deposition, contributing to fibrosis and organ dysfunction. However, in acute injury conditions, periostin was protective and promoted kidney repair by inhibiting epithelial cell death, inducing a differential macrophage polarization and promoting epithelial proliferation. The beneficial effect of periostin was maintained 6 weeks after AKI, with KO mice showing increased interstitial fibrosis and overexpressing mice displaying the opposite effect. Chronic fibrosis development after AKI was dependent on the initial injury response in this model. Besides, periostin alone did not induce spontaneous fibrosis after 4 months of chronic overexpression, further indicating that the distinctive functions of periostin in acute versus chronic conditions may depend on the different contexts and mechanisms implicated in these diseases.

In summary, our results demonstrate a novel protective role of periostin in AKI. This role is dual: i) periostin inhibits pro-apoptotic pathways and promotes proliferation of renal epithelial cells at least in part through direct interaction with Itg $\beta$ 1, favoring preservation of renal epithelium and a more efficient repair, and ii) periostin promotes a regenerative trophic macrophage phenotype during the repair phase of AKI, by driving proliferation of macrophages in the kidney and their secretion of pro-regenerative factors. These results position for the first time periostin in the repair mechanisms following AKI and contribute to our better understanding and more efficient design of AKI-targeted treatments.

#### **Author contributions**

R.K., N.P., C.E.C. and C.C. designed the study, analyzed data and prepared the manuscript.

R.K., N.P., P.K., S.P., S.V. and A.D. carried out experiments. J.C.D. provided scientific input. All authors approved the final version of the manuscript.

### **Acknowledgements and Financial Disclosures**

The authors thank the biochemical platform of the Centre de Recherche des Cordeliers for the measurements of renal function and the animal facility of INSERM UMRS 1155 for their valuable help with animal breeding. This work was supported by grants from the Agence Nationale de la Recherche (ANR), INSERM and INSERM-Transfert. Disclosures: None.

### **Supplemental material Table of Contents**

#### Supplemental Methods

- **Measurement of renal function**
- **Histological evaluation**
- **Western blotting**
- **Quantitative Real-time PCR**
- **Immunohistochemistry/Immunofluorescence**
- **In situ hybridization**
- **TUNEL assay**
- **Co-immunoprecipitation**

#### Supplemental Tables

- **Supplemental Table 1. PCR reaction and products used for the genotyping of the triple transgenic Pax8-rtTA/LC1-Cre/Tet-o-Periostin mice.**
- **Supplemental Table 2. Primer sequences used for quantitative Real-time PCR.**

## Supplemental Figure legends

- **Supplemental Figure 1. Co-localization of periostin with different renal tubular markers in WT mice 72h after I/R.**
- **Supplemental Figure 2. Kidney/body weight ratio of periostin-overexpressing and KO mice compared to their respective controls at basal conditions and 72h after I/R.**
- **Supplemental Figure 3. Periostin protects from apoptosis induction after I/R.**
- **Supplemental Figure 4. Periostin promotes proliferation of tubular cells after I/R.**
- **Supplemental Figure 5. Periostin inhibits the activation of the Itg $\beta$ 1 downstream targets FAK and ERK.**
- **Supplemental Figure 6. Periostin protects primary tubular cells from oxidative stress-induced cell death.**
- **Supplemental Figure 7. Recombinant periostin directly promotes the polarization and proliferation of cultured macrophages.**
- **Supplemental Figure 8. Chronic periostin overexpression is not linked to a profibrotic phenotype.**
- **Supplemental Figure 9. Periostin protects from fibrosis development 6w after I/R.**
- **Supplemental Figure 10. M2a markers are not increased in renal macrophages derived from periostin-overexpressing mice.**

## Supplemental Figures

## References

1. Bonventre JV, Yang L: Cellular pathophysiology of ischemic acute kidney injury. *J Clin Invest* 121: 4210-4221, 2011.
2. Basile DP, Anderson MD, Sutton TA: Pathophysiology of acute kidney injury. *Compr Physiol* 2: 1303-1353, 2012.
3. Grams ME, Rabb H: The distant organ effects of acute kidney injury. *Kidney Int* 81: 942-948, 2012.
4. Horiuchi K, Amizuka N, Takeshita S, Takamatsu H, Katsuura M, Ozawa H, et al.: Identification and characterization of a novel protein, periostin, with restricted expression to periosteum and periodontal ligament and increased expression by transforming growth factor beta. *J Bone Miner Res* 14: 1239-1249, 1999.
5. Prakoura N, Chatziantoniou C: Periostin in kidney diseases. *Cell Mol Life Sci* 74: 4315-4320, 2017.
6. Prakoura N, Chatziantoniou C: Matricellular Proteins and Organ Fibrosis. *Curr Pathobiol Rep* 5: 111-121, 2017.
7. Malanchi I, Santamaria-Martínez A, Susanto E, Peng H, Lehr HA, Delaloye JF, et al.: Interactions between cancer stem cells and their niche govern metastatic colonization. *Nature* 481: 85-89, 2011.
8. Norris RA, Damon B, Mironov V, Kasyanov V, Ramamurthi A, Moreno-Rodriguez R, et al.: Periostin regulates collagen fibrillogenesis and the biomechanical properties of connective tissues. *J Cell Biochem* 101: 695-711, 2007.
9. Kii I, Nishiyama T, Li M, Matsumoto K, Saito M, Amizuka N, et al.: Incorporation of tenascin-C into the extracellular matrix by periostin underlies an extracellular meshwork architecture. *J Biol Chem* 285: 2028-2039, 2010.

10. Snider P, Hinton RB, Moreno-Rodriguez RA, Wang J, Rogers R, Lindsley A, et al.: Periostin is required for maturation and extracellular matrix stabilization of noncardiomyocyte lineages of the heart. *Circ Res* 102: 752-760, 2008.
11. Gillan L, Matei D, Fishman DA, Gerbin CS, Karlan BY, Chang DD: Periostin secreted by epithelial ovarian carcinoma is a ligand for alpha(V)beta(3) and alpha(V)beta(5) integrins and promotes cell motility. *Cancer Res* 62: 5358-5364, 2002.
12. Li G, Jin R, Norris RA, Zhang L, Yu S, Wu F, et al.: Periostin mediates vascular smooth muscle cell migration through the integrins alphavbeta3 and alphavbeta5 and focal adhesion kinase (FAK) pathway. *Atherosclerosis* 208: 358-365, 2010.
13. Lambert AW, Wong CK, Ozturk S, Papageorgis P, Raghunathan R, Alekseyev Y, et al.: Tumor Cell-Derived Periostin Regulates Cytokines That Maintain Breast Cancer Stem Cells. *Mol Cancer Res* 14: 103-113, 2016.
14. Li L, Fan D, Wang C, Wang JY, Cui XB, Wu D, et al.: Angiotensin II increases periostin expression via Ras/p38 MAPK/CREB and ERK1/2/TGF- $\beta$ 1 pathways in cardiac fibroblasts. *Cardiovasc Res* 91: 80-89, 2011.
15. Zhao X, Hao J, Duan H, Rong Z, Li F: Phosphoinositide 3-kinase/protein kinase B/periostin mediated platelet-derived growth factor-induced cell proliferation and extracellular matrix production in lupus nephritis. *Exp Biol Med (Maywood)* 242: 160-168, 2017.
16. Takayama G, Arima K, Kanaji T, Toda S, Tanaka H, Shoji S, et al.: Periostin: a novel component of subepithelial fibrosis of bronchial asthma downstream of IL-4 and IL-13 signals. *J Allergy Clin Immunol* 118: 98-104, 2006.

17. Masuoka M, Shiraishi H, Ohta S, Suzuki S, Arima K, Aoki S, et al.: Periostin promotes chronic allergic inflammation in response to Th2 cytokines. *J Clin Invest* 122: 2590-2600, 2012.
18. Prakoura N, Kavvadas P, Kormann R, Dussaule JC, Chadjichristos CE, Chatziantoniou C: NFκB-Induced Periostin Activates Integrin-β3 Signaling to Promote Renal Injury in GN. *J Am Soc Nephrol* 28: 1475-1490, 2017.
19. Prakoura N, Chatziantoniou C: Periostin and Discoidin Domain Receptor 1: New Biomarkers or Targets for Therapy of Renal Disease. *Front Med (Lausanne)* 4: 52, 2017.
20. Mael-Ainin M, Abed A, Conway SJ, Dussaule JC, Chatziantoniou C: Inhibition of periostin expression protects against the development of renal inflammation and fibrosis. *J Am Soc Nephrol* 25: 1724-1736, 2014.
21. Koesters R, Kaissling B, Lehir M, Picard N, Theilig F, Gebhardt R, et al.: Tubular overexpression of transforming growth factor-beta1 induces autophagy and fibrosis but not mesenchymal transition of renal epithelial cells. *Am J Pathol* 177: 632-643, 2010.
22. Zhang D, Liu Y, Wei Q, Huo Y, Liu K, Liu F, et al.: Tubular p53 regulates multiple genes to mediate AKI. *J Am Soc Nephrol* 25: 2278-2289, 2014.
23. Wei Q, Dong G, Chen JK, Ramesh G, Dong Z: Bax and Bak have critical roles in ischemic acute kidney injury in global and proximal tubule-specific knockout mouse models. *Kidney Int* 84: 138-148, 2013.
24. Hakuno D, Kimura N, Yoshioka M, Mukai M, Kimura T, Okada Y, et al.: Periostin advances atherosclerotic and rheumatic cardiac valve degeneration by inducing

- angiogenesis and MMP production in humans and rodents. *J Clin Invest* 120: 2292-2306, 2010.
25. Ghatak S, Misra S, Norris RA, Moreno-Rodriguez RA, Hoffman S, Levine RA, et al.: Periostin induces intracellular cross-talk between kinases and hyaluronan in atrioventricular valvulogenesis. *J Biol Chem* 289: 8545-8561, 2014.
26. Matsuzawa M, Arai C, Nomura Y, Murata T, Yamakoshi Y, Oida S, et al.: Periostin of human periodontal ligament fibroblasts promotes migration of human mesenchymal stem cell through the  $\alpha\text{v}\beta\text{3}$  integrin/FAK/PI3K/Akt pathway. *J Periodontal Res* 50: 855-863, 2015.
27. Ying Y, Kim J, Westphal SN, Long KE, Padanilam BJ: Targeted deletion of p53 in the proximal tubule prevents ischemic renal injury. *J Am Soc Nephrol* 25: 2707-2716, 2014.
28. Ferenbach DA, Bonventre JV: Mechanisms of maladaptive repair after AKI leading to accelerated kidney ageing and CKD. *Nat Rev Nephrol* 11: 264-276, 2015.
29. Yang L, Besschetnova TY, Brooks CR, Shah JV, Bonventre JV: Epithelial cell cycle arrest in G2/M mediates kidney fibrosis after injury. *Nat Med* 16: 535-543, 2010.
30. Nishioka S, Nakano D, Kitada K, Sofue T, Ohsaki H, Moriwaki K, Hara T, Ohmori K, Kohno M, Nishiyama A. The cyclin-dependent kinase inhibitor p21 is essential for the beneficial effects of renal ischemic preconditioning on renal ischemia/reperfusion injury in mice. *Kidney Int* 85: 871-879, 2014.
31. DiRocco DP, Bisi J, Roberts P, Strum J, Wong KK, Sharpless N, Humphreys BD. CDK4/6 inhibition induces epithelial cell cycle arrest and ameliorates acute kidney injury. *Am J Physiol Renal Physiol* 306: F379-388, 2014.

32. Humphreys BD, Valerius MT, Kobayashi A, Mugford JW, Soeung S, Duffield JS, et al.: Intrinsic epithelial cells repair the kidney after injury. *Cell Stem Cell* 2: 284-291, 2008.
33. Moreno-Layseca P, Streuli CH: Signalling pathways linking integrins with cell cycle progression. *Matrix Biol* 34: 144-153, 2014.
34. Rozo M, Li L, Fan CM: Targeting  $\beta$ 1-integrin signaling enhances regeneration in aged and dystrophic muscle in mice. *Nat Med* 22: 889-896, 2016.
35. Taylor WR, Stark GR: Regulation of the G2/M transition by p53. *Oncogene* 20: 1803-1815, 2001.
36. Bunz F, Dutriaux A, Lengauer C, Waldman T, Zhou S, Brown JP, et al.: Requirement for p53 and p21 to sustain G2 arrest after DNA damage. *Science* 282: 1497-1501, 1998.
37. Norbury C, Blow J, Nurse P: Regulatory phosphorylation of the p34cdc2 protein kinase in vertebrates. *EMBO J* 10: 3321-3329, 1991.
38. An JN, Yang SH, Kim YC, Hwang JH, Park JY, Kim DK, Kim JH, Kim DW, Hur DG, Oh YK, Lim CS, Kim YS, Lee JP. Periostin induces kidney fibrosis after acute kidney injury via the p38 MAPK pathway. *Am J Physiol Renal Physiol* 316: F426-F437, 2019.
39. Forbes SJ, Rosenthal N: Preparing the ground for tissue regeneration: from mechanism to therapy. *Nat Med* 20: 857-869, 2014.
40. Lech M, Anders HJ: Macrophages and fibrosis: How resident and infiltrating mononuclear phagocytes orchestrate all phases of tissue injury and repair. *Biochim Biophys Acta* 1832: 989-997, 2013.
41. Lech M, Gröbmayer R, Weidenbusch M, Anders HJ: Tissues use resident dendritic cells and macrophages to maintain homeostasis and to regain homeostasis upon tissue injury: the immunoregulatory role of changing tissue environments. *Mediators Inflamm* 2012: 951390, 2012.

42. Lee S, Huen S, Nishio H, Nishio S, Lee HK, Choi BS, et al.: Distinct macrophage phenotypes contribute to kidney injury and repair. *J Am Soc Nephrol* 22: 317-326, 2011.
43. Zhou W, Ke SQ, Huang Z, Flavahan W, Fang X, Paul J, et al.: Periostin secreted by glioblastoma stem cells recruits M2 tumour-associated macrophages and promotes malignant growth. *Nat Cell Biol* 17: 170-182, 2015.
44. Jenkins SJ, Ruckerl D, Cook PC, Jones LH, Finkelman FD, van Rooijen N, et al.: Local macrophage proliferation, rather than recruitment from the blood, is a signature of TH2 inflammation. *Science* 332: 1284-1288, 2011.
45. Jenkins SJ, Ruckerl D, Thomas GD, Hewitson JP, Duncan S, Brombacher F, et al.: IL-4 directly signals tissue-resident macrophages to proliferate beyond homeostatic levels controlled by CSF-1. *J Exp Med* 210: 2477-2491, 2013.
46. Wang Y, Chang J, Yao B, Niu A, Kelly E, Breeggemann MC, et al.: Proximal tubule-derived colony stimulating factor-1 mediates polarization of renal macrophages and dendritic cells, and recovery in acute kidney injury. *Kidney Int* 88: 1274-1282, 2015.
47. Capote J, Kramerova I, Martinez L, Vetrone S, Barton ER, Sweeney HL, et al.: Osteopontin ablation ameliorates muscular dystrophy by shifting macrophages to a pro-regenerative phenotype. *J Cell Biol* 213: 275-288, 2016.
48. Yoshino J, Monkawa T, Tsuji M, Hayashi M, Saruta T: Leukemia inhibitory factor is involved in tubular regeneration after experimental acute renal failure. *J Am Soc Nephrol* 14: 3090-3101, 2003.

## Figure legends

### Figure 1

**Periostin is strongly expressed at the repair phase of I/R by renal epithelial cells.** (A, B) Periostin mRNA (A) and protein expression (B) is gradually upregulated towards the repair phase of I/R. (C) Periostin is localized in the tubulointerstitial parenchyma around injured and dilated tubules after I/R in WT mice, showing no expression in KO mice. (D) Periostin is produced by renal tubular cells after I/R, as revealed by in situ hybridization staining. (E) Scheme of triple transgenic construct used to overexpress periostin in renal epithelial cells. The reverse tetracycline-dependent transactivator (rtTA) drives the expression of Cre recombinase specifically in the renal tubular compartment (controlled by Pax8 promoter) after doxycycline administration. Cre recombinase excises lacZ and approaches periostin to the TRE promoter which is expressed in response to doxycycline. (F) Periostin is significantly increased 72h after I/R in control mice, while it is stably upregulated in periostin-overexpressing mice. (G) Periostin is secreted around injured tubules at the repair phase of I/R (72h) in control mice, showing a similar localization in overexpressing mice at all time points. Representative images are shown. Scale bars: 50  $\mu$ m (C, D), 100  $\mu$ m (G). \* $P$ <0.05, \*\* $P$ <0.01 vs. CNT, # $P$ <0.05 vs. CNT I/R 24h.  $n$ =3 for CNT and 6 per I/R group.

## Figure 2

### **Periostin overexpression protects from renal structural and functional damage after I/R.**

(A, B) PAS staining showing decreased epithelial damage in periostin-overexpressing mice at both 24h (A) and 72h (B) after I/R. (C, D) Tubular necrosis (C) and tubular dilation (D), depicted in quantification graphs, are decreased in periostin-overexpressing mice after I/R. (E, F) Plasma creatinine (E) and plasma urea (F) are attenuated in periostin-overexpressing mice at both I/R time points. (G-K) Kidney injury markers NGAL (G) and KIM-1 (H), as well as pro-inflammatory mediators IL-6 (I), MCP-1 (J) and VCAM-1 (K) show reduced expression levels in periostin-overexpressing mice after I/R. The mRNA expression levels are presented

relatively to basal control levels. (L) Tubular KIM-1 staining is significantly lower in periostin-overexpressing mice 72h after I/R. Representative images are shown. Scale bars: 100  $\mu$ m (A, B), 200  $\mu$ m (L). \* $P$ <0.05, \*\* $P$ <0.01, \*\*\* $P$ <0.001 vs. CNT or POSTN, # $P$ <0.05, ## $P$ <0.01, ### $P$ <0.001 vs. CNT I/R 24h or CNT I/R 72h,  $^{\S}$  $P$ <0.05,  $^{\S\S}$  $P$ <0.01 vs. I/R 24h.  $n$ =3 for CNT and 5-6 per I/R group.

### Figure 3

**Periostin deletion exacerbates renal structural and functional damage after I/R.** (A, B) PAS staining (A) and tubular injury score (B) depicting increased epithelial damage in periostin KO mice at both 24h and 72h after I/R. (C, D) Plasma urea (C) and plasma creatinine (D) are increased in periostin KO mice after I/R. (E, F) Injury markers NGAL (E) and KIM-1 (F) show increased expression levels in periostin KO mice at the injury phase of I/R. (G) Tubular KIM-1 staining is significantly higher in periostin KO mice after I/R. CTL stands for control contralateral kidney. Representative images are shown. Scale bars: 100  $\mu$ m. \* $P$ <0.05, \*\* $P$ <0.01 vs. CTL, # $P$ <0.05, ## $P$ <0.01 vs. WT I/R 24h or WT I/R 72h.  $n$ =3 for CTL and 7-8 per I/R group.

### Figure 4

**Periostin protects from cell cycle arrest and apoptosis after I/R.** (A, B) The expression levels of the cell cycle arrest mediators p21 (A) and p16 (B) is highly attenuated in periostin-overexpressing mice after I/R. mRNA expression is presented relatively to basal control levels. (C, D) Western blots of p21 and p-JNK and their quantifications showing decreased protein levels in periostin-overexpressing mice after I/R. (E) Cell death, assessed by TUNEL staining, is reduced in periostin-overexpressing mice after I/R. (F) TUNEL staining showing

increased cell death in periostin KO mice after I/R. (G, H) Western blots (G) and quantifications (H) of p-AKT, p53, p21 and BAX, showing decreased protein levels of p-AKT and increased levels of p53, p21 and BAX in periostin KO compared to WT mice after I/R. Representative images are shown. Scale bars: 100  $\mu\text{m}$  (E), 50  $\mu\text{m}$  (F). \* $P$ <0.05, \*\* $P$ <0.01, \*\*\* $P$ <0.001 vs. CNT or CTL, # $P$ <0.05, ## $P$ <0.01, ### $P$ <0.001 vs. CNT I/R or WT I/R, § $P$ <0.05 vs. I/R 24h.  $n$ =4 for CNT or CTL and 5-7 per I/R group.

### Figure 5

**Periostin interacts with integrin- $\beta$ 1 on epithelial cells after I/R.** (A-C) Itg $\beta$ 1 is gradually upregulated in tubular epithelial cells after I/R (A), while its levels are similarly induced in control and periostin-overexpressing mice (B) or WT and periostin KO mice (C). (D) Co-immunoprecipitation with an Itg $\beta$ 1 antibody showed that Itg $\beta$ 1 interacts with periostin after I/R. Representative images are shown. Scale bars: 50  $\mu\text{m}$ . \* $P$ <0.05, \*\* $P$ <0.01, \*\*\* $P$ <0.001 vs. CNT, POSTN, WT or KO, § $P$ <0.05, §§ $P$ <0.01 vs. I/R 24h.  $n$ =4 for CNT or CTL and 6 per I/R group.

### Figure 6

**Periostin inhibits hypoxia-induced cell death of primary tubular cells through interaction with integrin- $\beta$ 1.** (A) Cultured primary tubular cells from control mice gradually overexpress periostin after mineral oil-induced hypoxia to a similar level with cells from periostin-overexpressing mice, while Itg $\beta$ 1 expression remains stable. (B) Co-immunofluorescence staining of Itg $\beta$ 1 and periostin in normoxia conditions and after 1h or 24h of mineral-oil induced hypoxia. The interaction pattern of control epithelial cells mediated by Itg $\beta$ 1 is lost after hypoxia, while it is markedly preserved in periostin-overexpressing cells. (C) Cell death,

assessed by TUNEL, is reduced in tubular cells overexpressing periostin at both early and late reoxygenation intervals after hypoxia. (D, E) Western blots and quantifications of cell cycle arrest and apoptosis mediators, showing blunted expression in periostin-overexpressing cells after hypoxia. (F) Western blot and quantification of Itgβ1 expression in primary tubular cells treated with control or Itgβ1 siRNA, showing efficient inhibition of Itgβ1 protein synthesis in Itgβ1 siRNA-treated cells. (G) Itgβ1 silencing increases the LDH release, indicative of cell death, of both control and periostin-overexpressing tubular cells after hypoxia, while periostin-overexpressing cells demonstrate highly decreased LDH release both before and after Itgβ1 silencing, compared to control cells. Representative images are shown. Scale bars: 100 μm. \* $P < 0.05$ , \*\* $P < 0.01$ , \*\*\* $P < 0.001$  vs. Normoxia, # $P < 0.05$ , ## $P < 0.01$  vs. CNT H/R 1h, CNT H/R 24h, CNT H/R Control siRNA or CNT H/R Itgβ1 siRNA, §§ $P < 0.01$ , §§§ $P < 0.001$  vs. H/R Control siRNA. Quantifications of 2-3 independent experiments performed in duplicates or triplicates are shown.

## Figure 7

**Periostin promotes proliferation of macrophages in the kidney.** (A) F4/80 staining and quantification show a higher abundance of macrophages in the kidneys of periostin-overexpressing mice after I/R. (B, C) MCM2 (green)-F4/80 (red) (B) and PCNA (red)-F4/80 (green) (C) co-staining 72h after I/R and quantification of the number of the MCM2+ or PCNA+ macrophages reveal increased proliferation of macrophages in periostin-overexpressing mice. (D, E) F4/80 staining (D) and quantification (E) show a lower abundance of kidney macrophages in periostin KO mice after I/R. (F) MCM2 (green)-F4/80 (red) co-staining 72h after I/R and quantification of the number of the MCM2+ macrophages reveal decreased proliferation of macrophages in periostin KO mice. Arrowheads indicate MCM2+

or PCNA+ macrophages. Representative images are shown. Scale bars: 100  $\mu\text{m}$  (A, D), 50  $\mu\text{m}$  (B, C, F). \* $P < 0.05$  vs. CNT, POSTN or CTL, # $P < 0.05$ , ### $P < 0.01$  vs. CNT I/R or WT I/R.  $n = 3$  for CNT or CTL and 6 per I/R group.

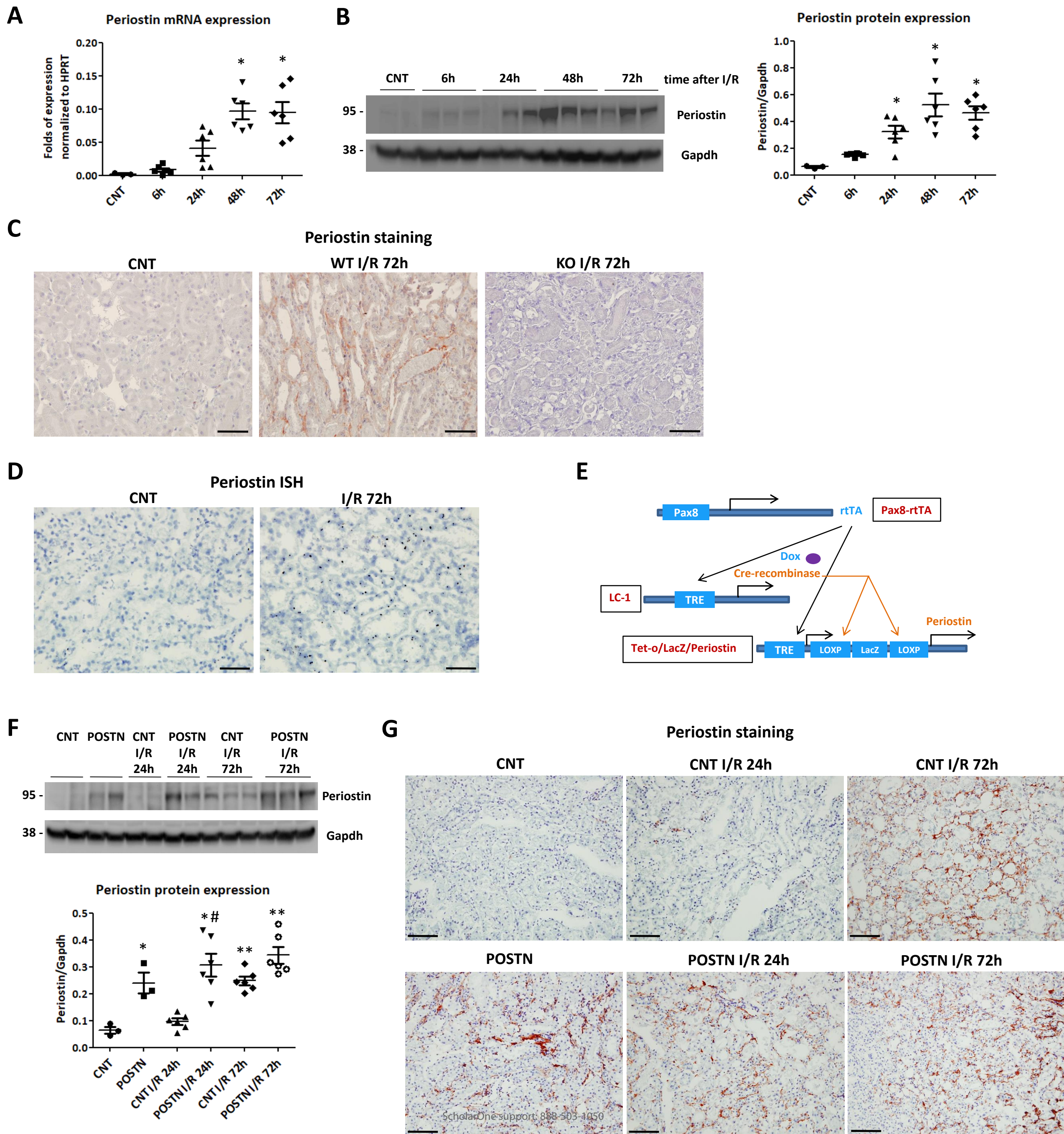
## Figure 8

### Periostin promotes polarization of kidney macrophages to a pro-regenerative phenotype.

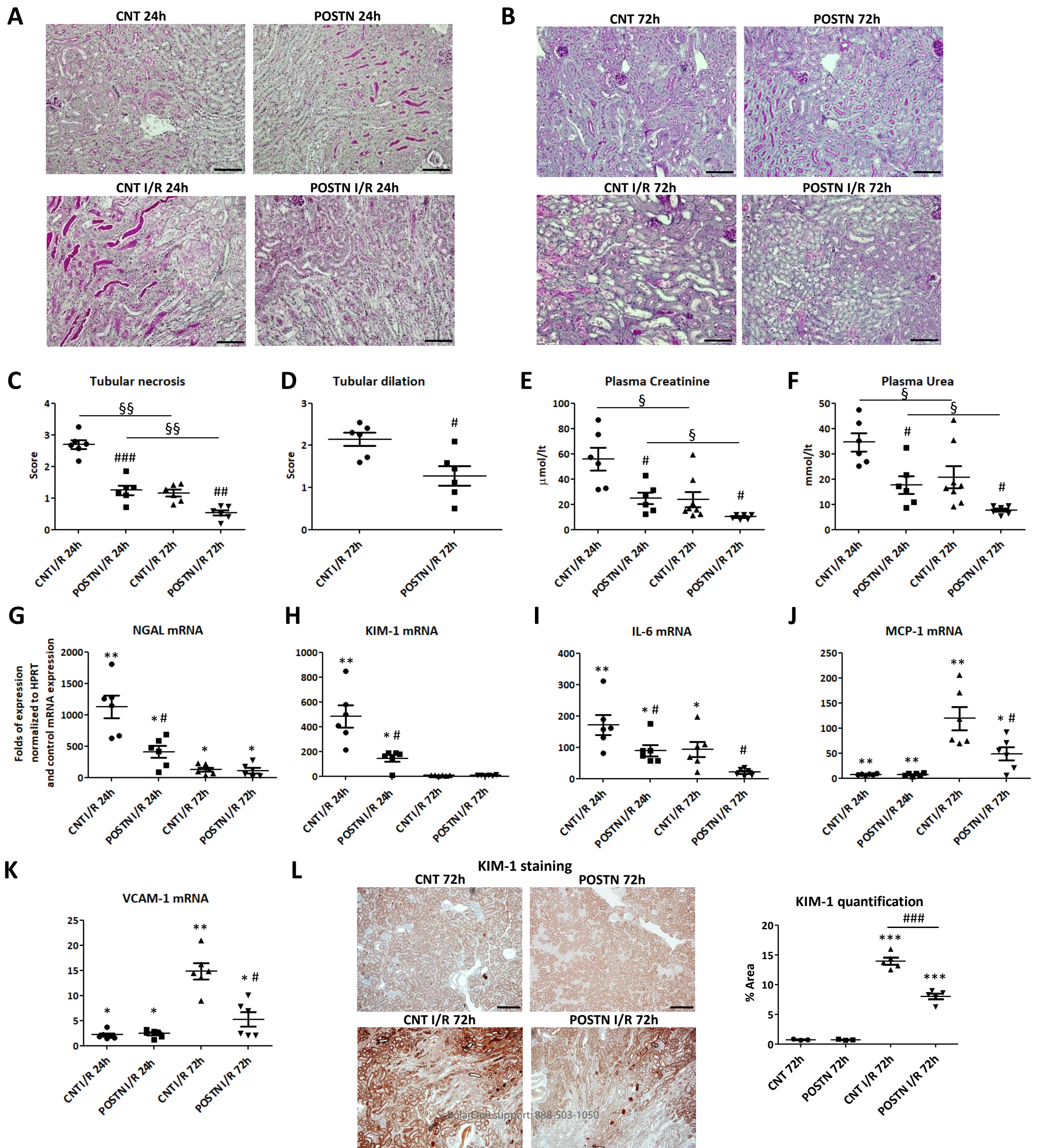
(A) mRNA expression of different markers in F4/80+ macrophages isolated from control and periostin-overexpressing mice 72h after I/R. Macrophages from periostin-overexpressing mice show decreased levels of IL-6 and higher levels of CD163, IL-10, CSF-1, uPA and LIF, indicating a polarization to a M2c regenerative phenotype. (B) Western blots and quantifications of different proteins in F4/80+ macrophages 72h after I/R. Macrophages from periostin-overexpressing mice produce higher levels of CD163, a M2c marker, and the trophic pro-regenerative factors LIF and uPA. (C, D) CD206+ macrophages in the kidney (C) and IL-10 expression levels in isolated renal macrophages (D) are lower in periostin KO mice after I/R, showing a decreased M2 polarization. (E) mRNA expression of different factors in RAW macrophages co-cultured with primary tubular cells for 48h at normal conditions (normoxia) or after subjection of cells to mineral oil-induced hypoxia. RAW macrophages co-cultured with periostin-overexpressing tubular cells express lower levels of IL-6 and higher levels of HB-EGF, uPA and LIF, only after co-culture with cells subjected to hypoxia. (F) Macrophages show increased protein production of uPA and LIF after co-culture with periostin-overexpressing tubular cells subjected to hypoxia, compared to co-culture with control cells. (G) p-H3 staining and quantification, showing a higher induction in the proliferation of macrophages after co-culture with hypoxia-treated tubular cells overexpressing periostin. Representative images are shown. Scale bars: 100  $\mu\text{m}$ . \* $P < 0.05$ ,

\*\* $P < 0.01$  vs. RAW, # $P < 0.05$ , ## $P < 0.01$  vs. CNT I/R, WT I/R or RAW + Cnt tubules.  $n = 5$  mice per group. For cell cultures, quantifications of 2-3 independent experiments performed in duplicates or triplicates are shown.

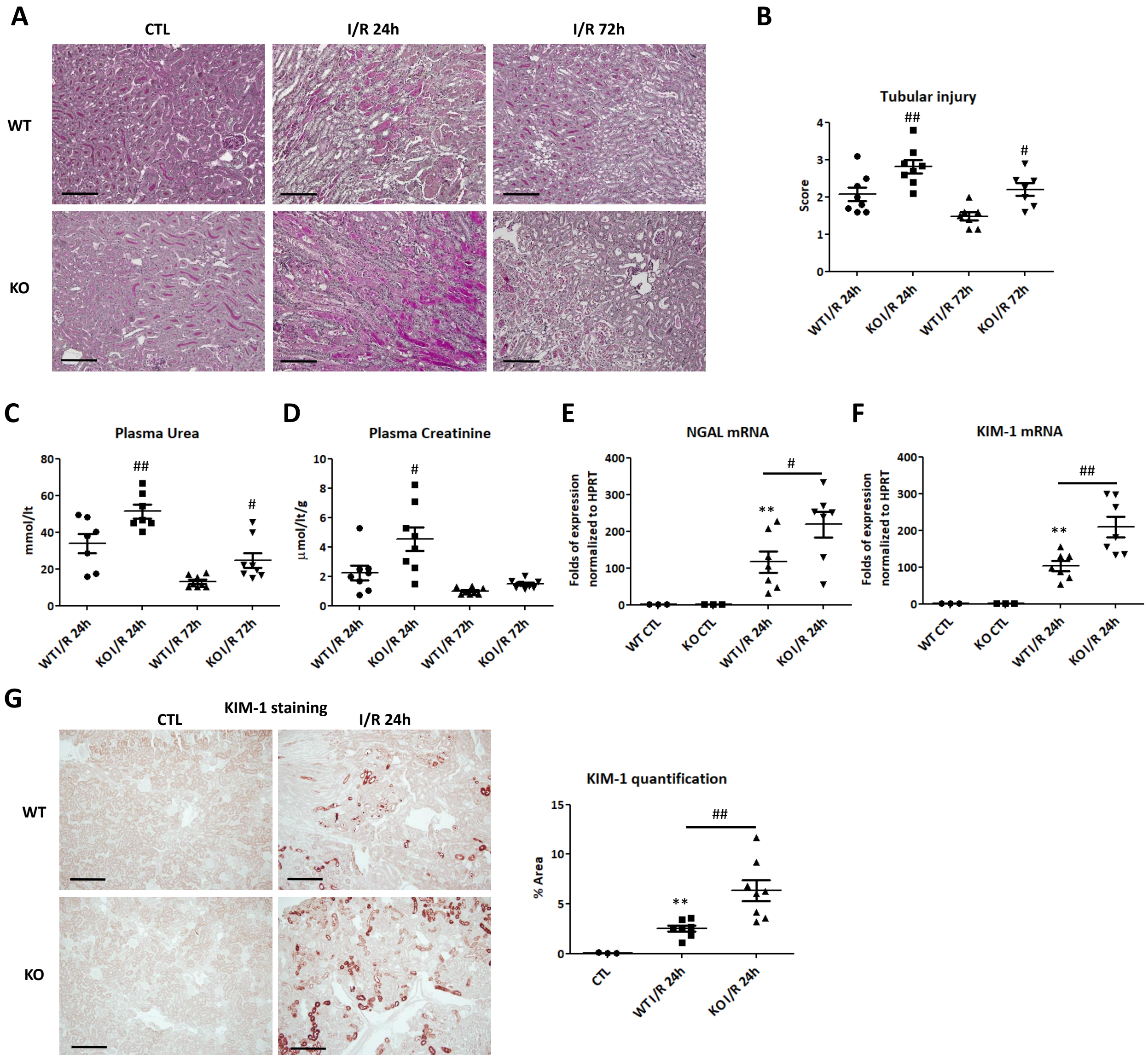
## Figure 1



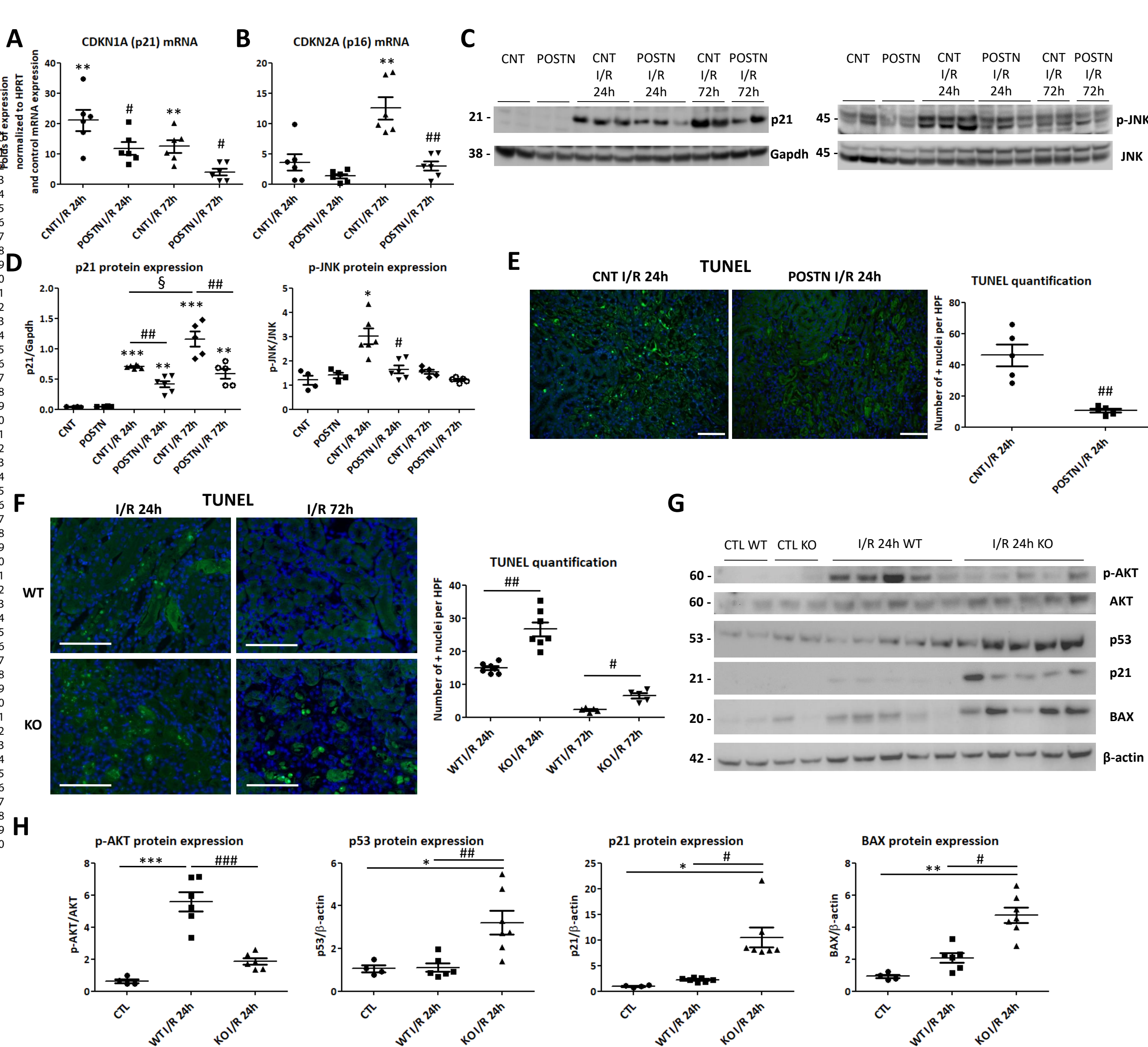
## Figure 2

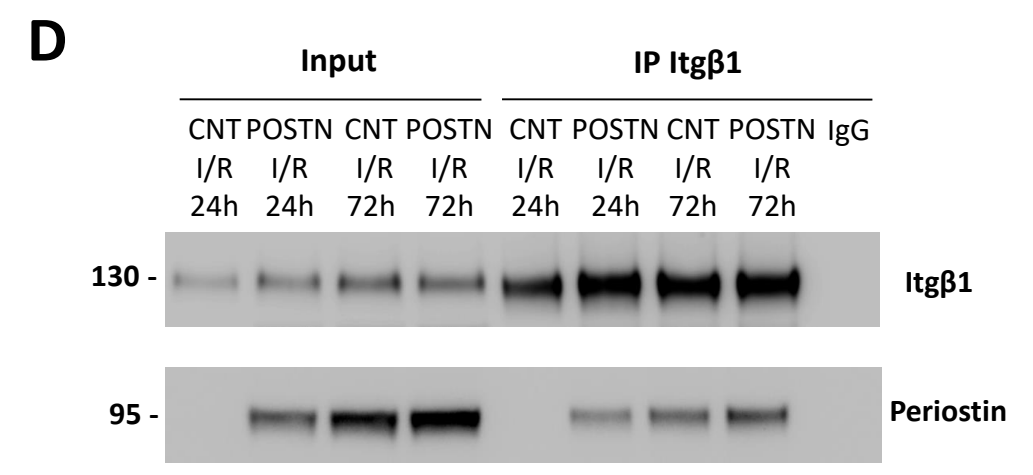
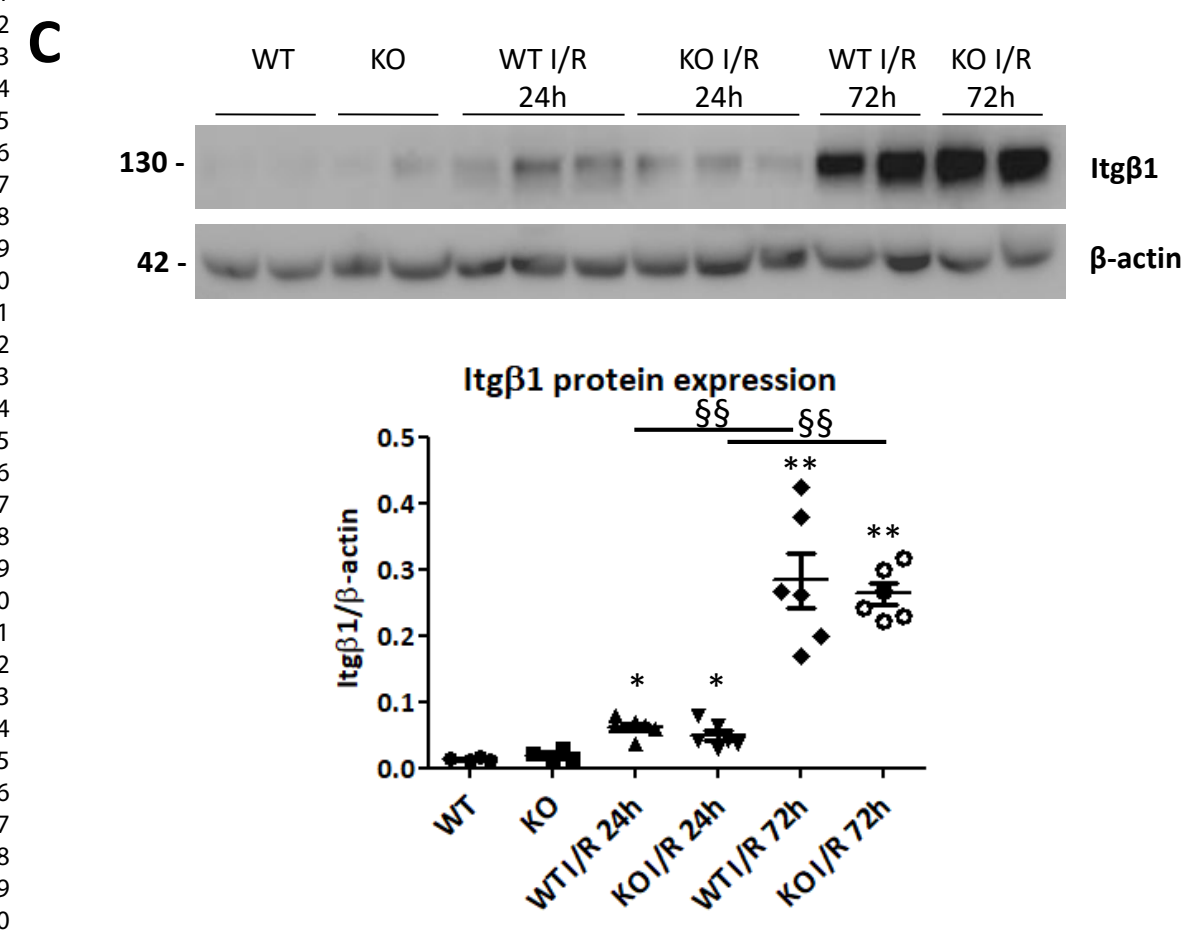
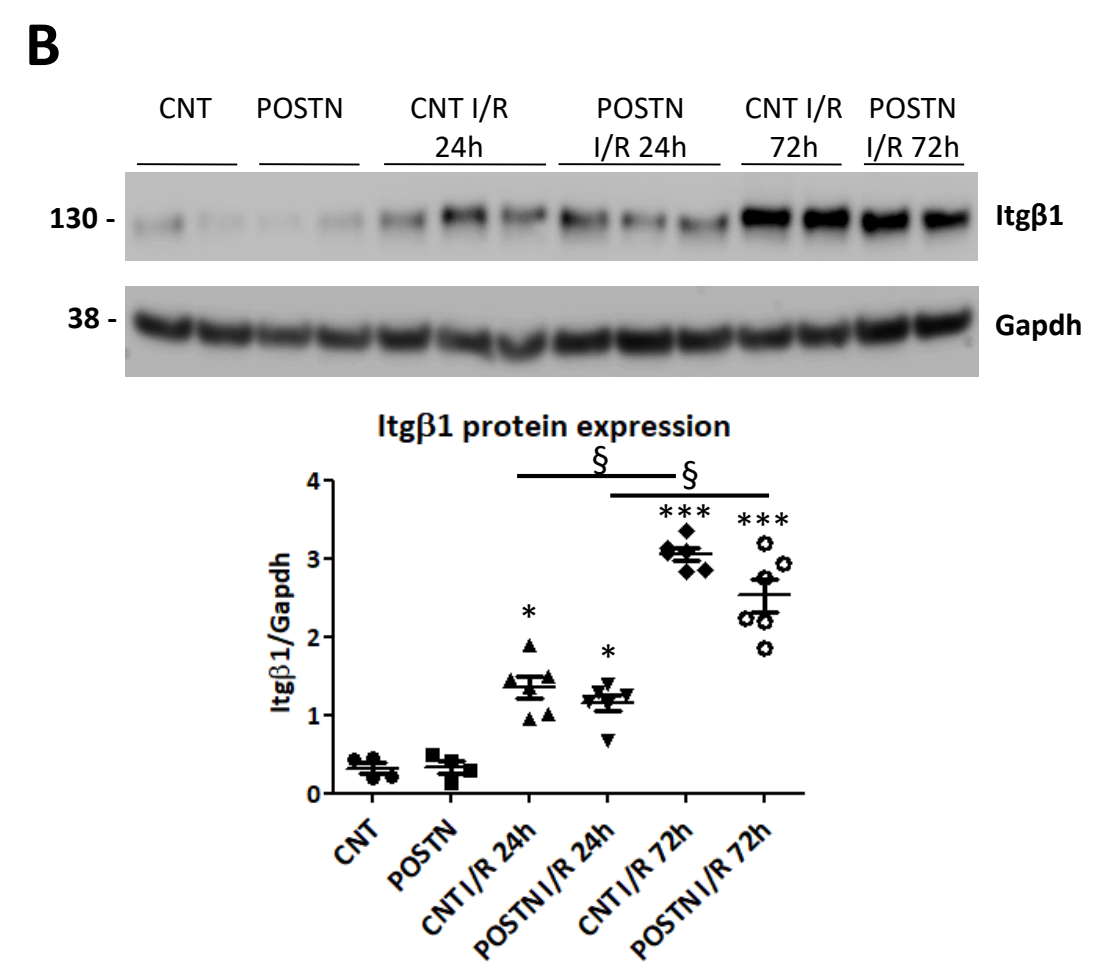
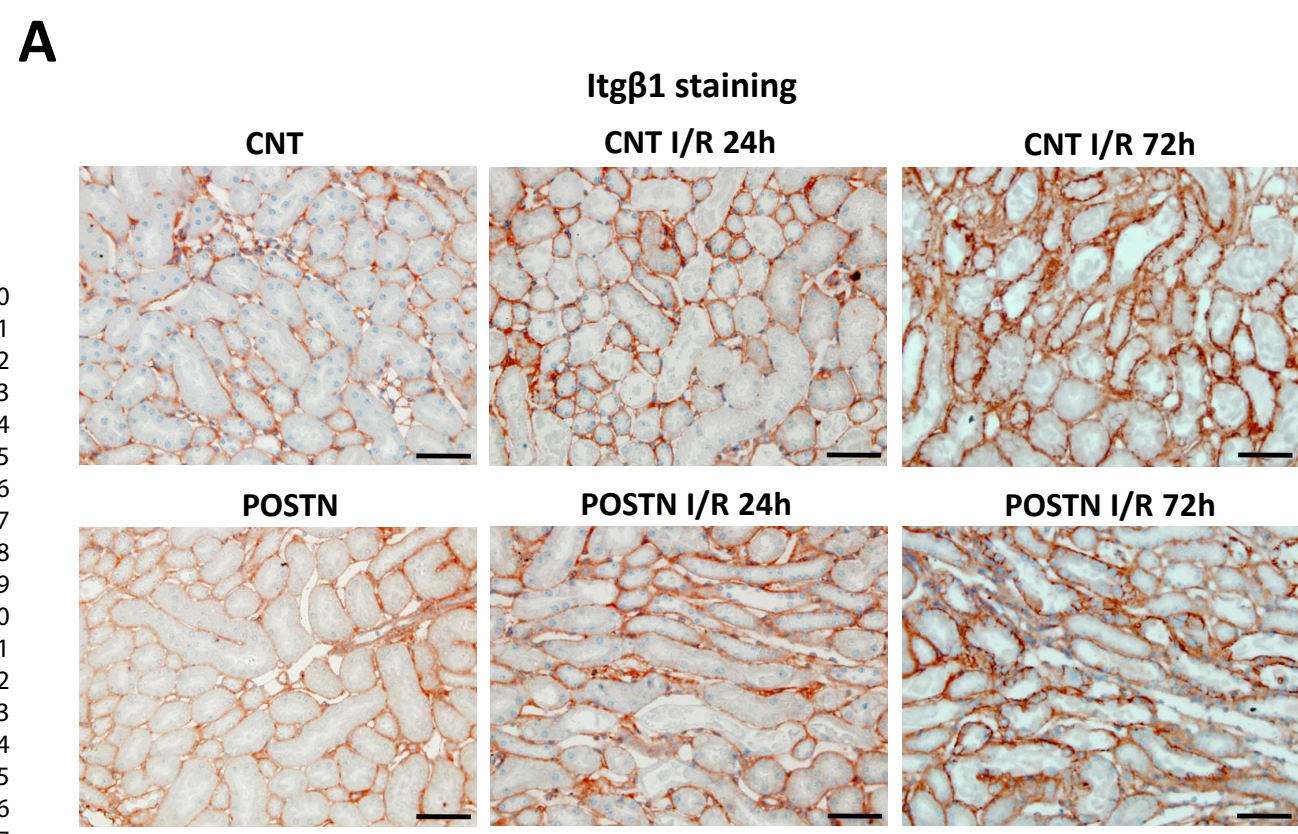


## Figure 3

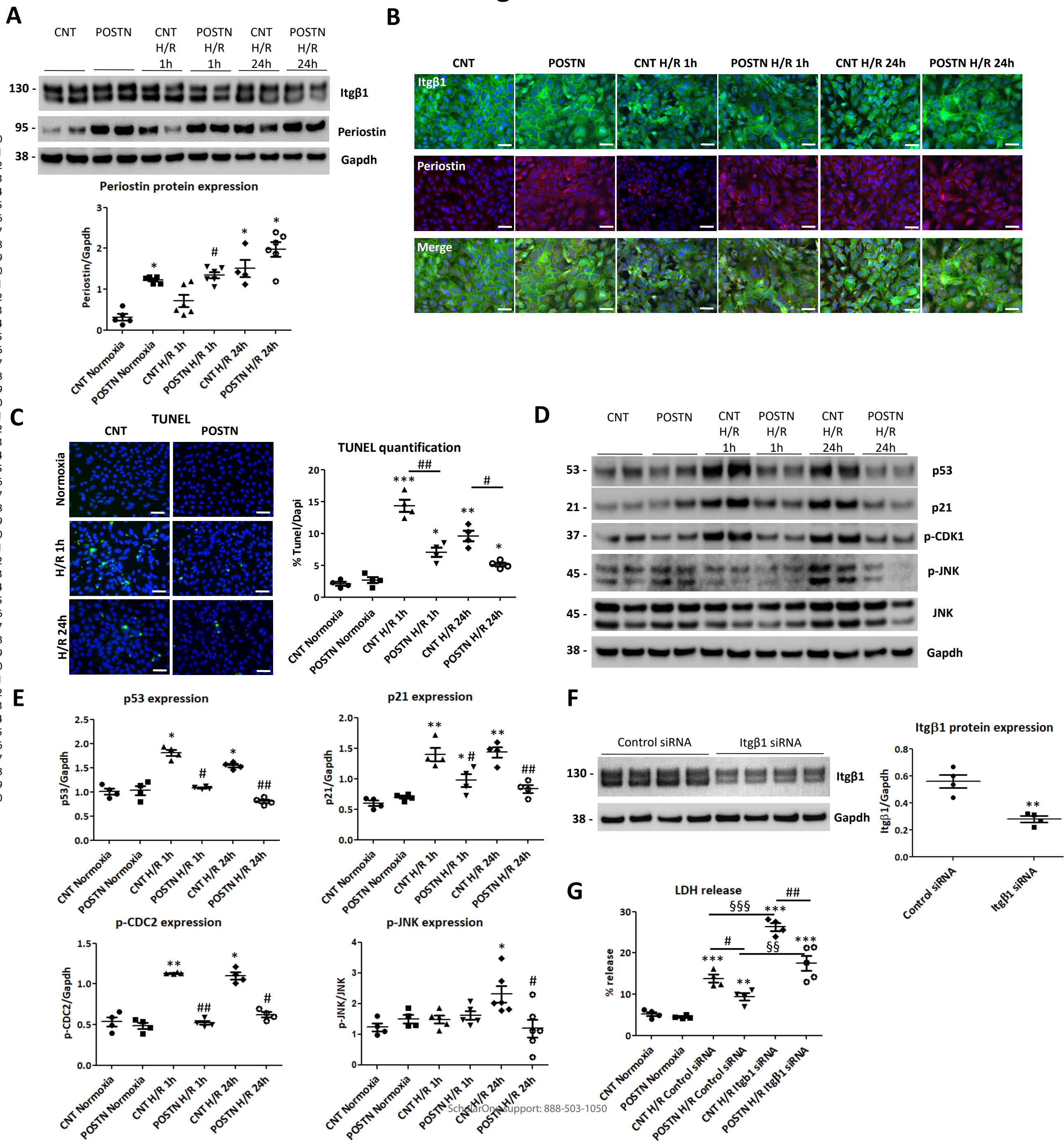


## Figure 4

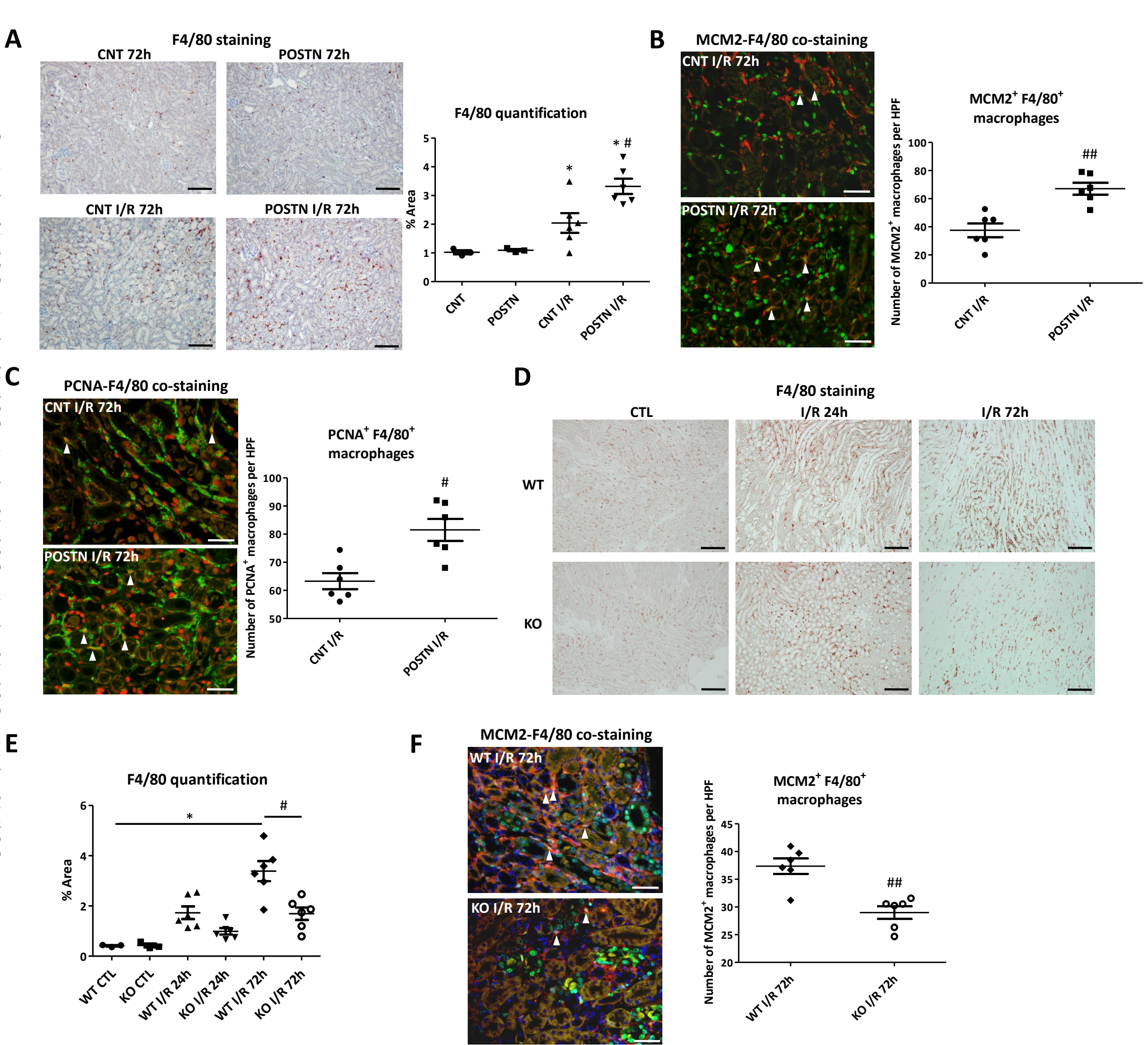




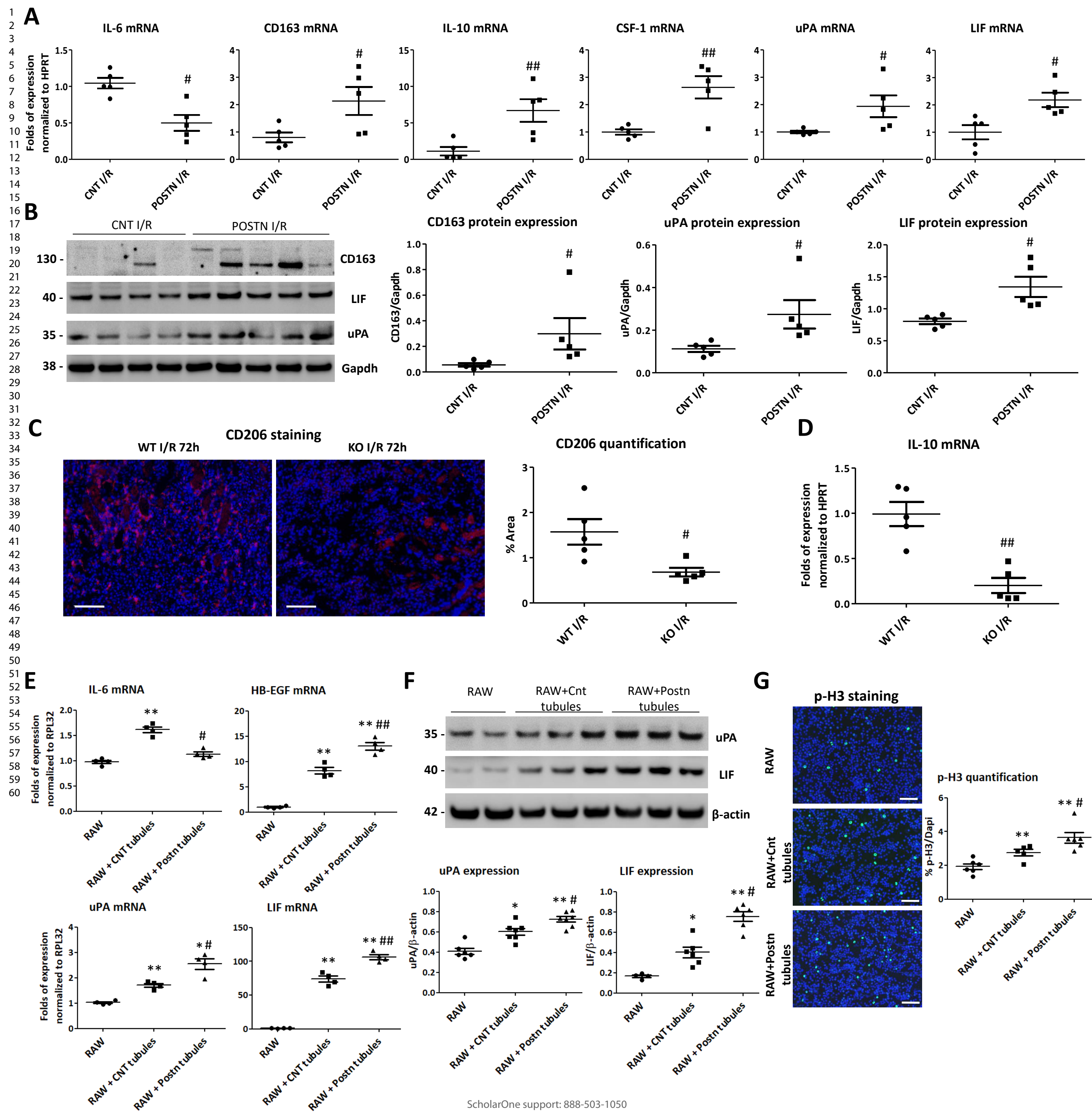
## Figure 6

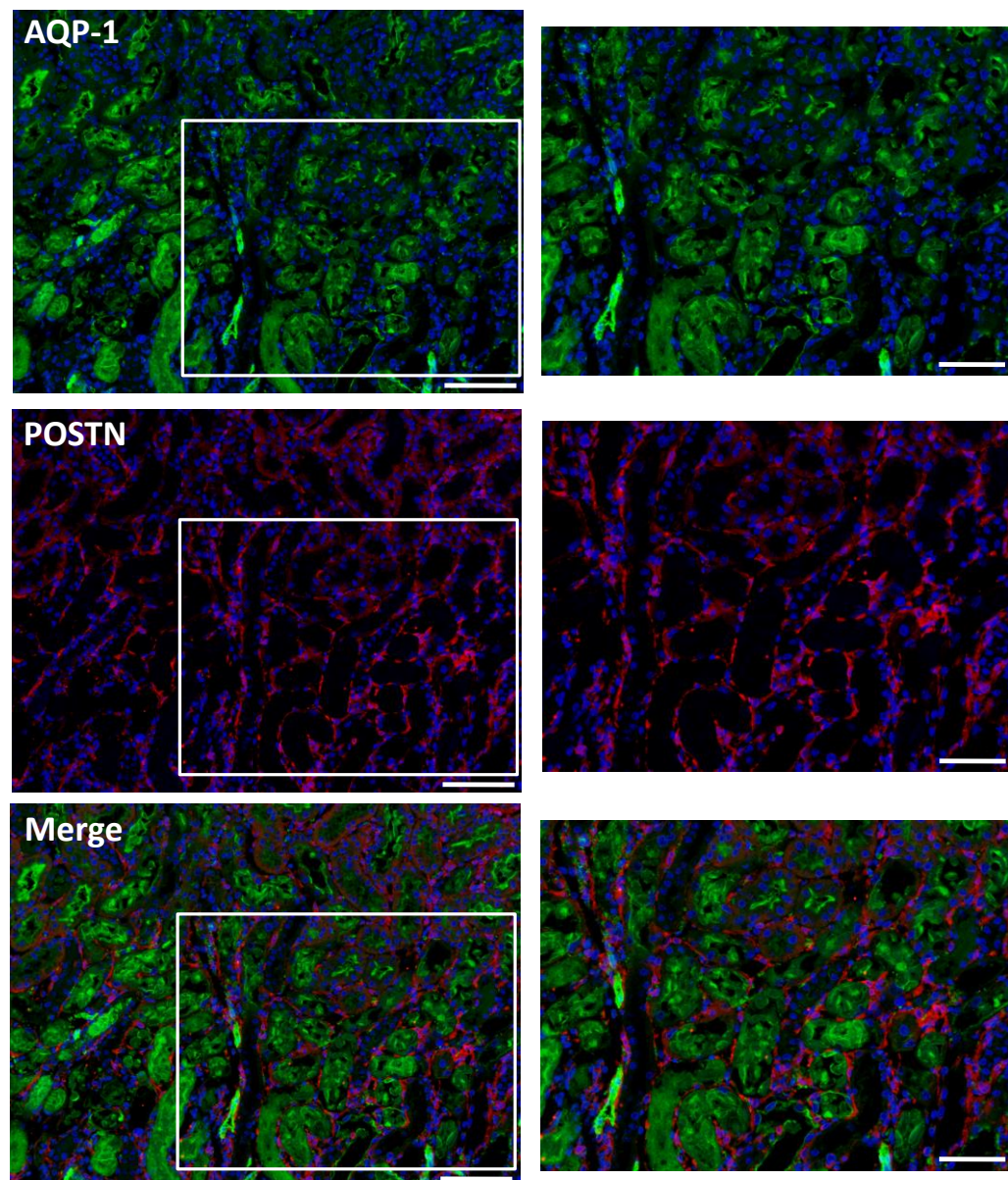
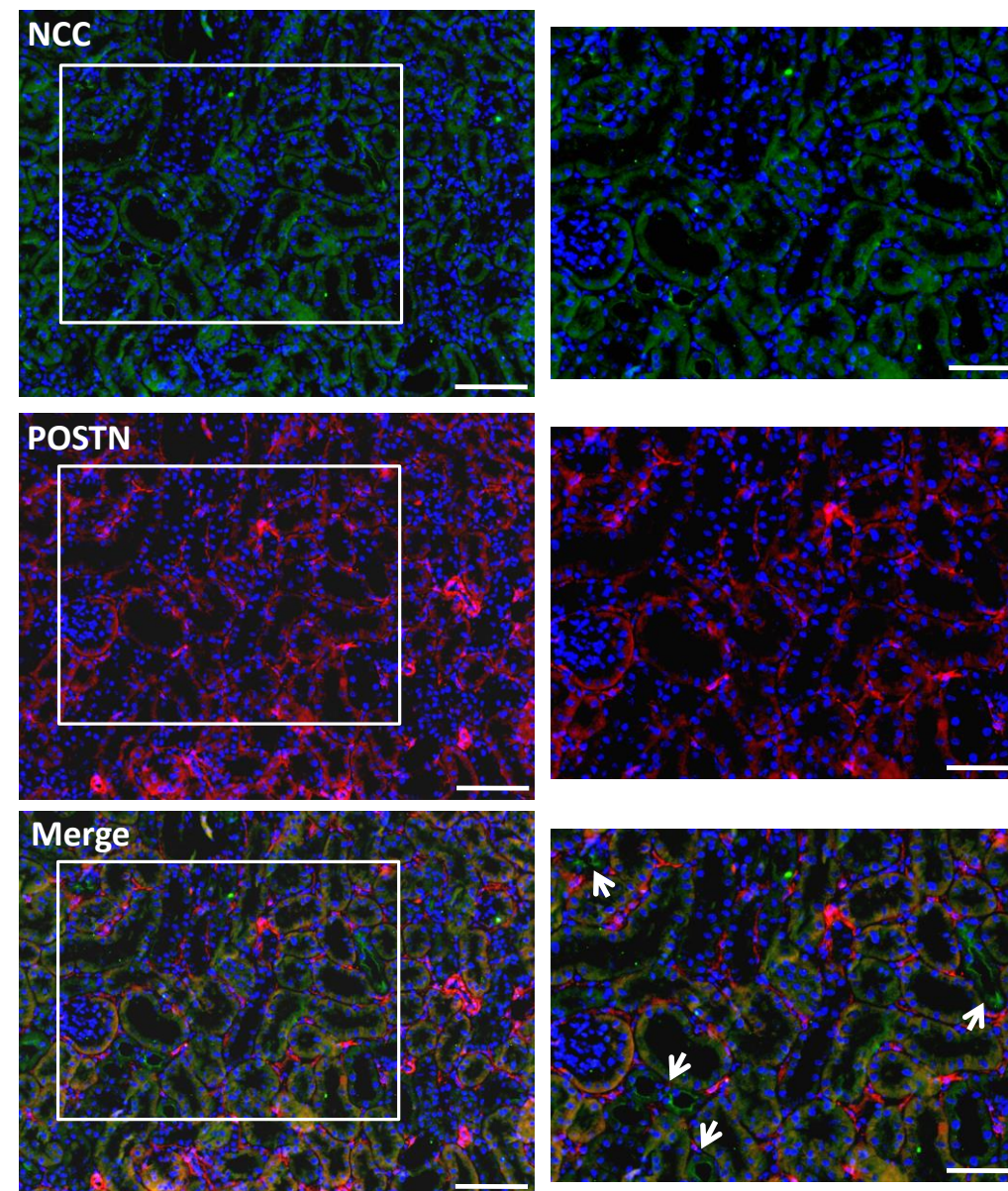
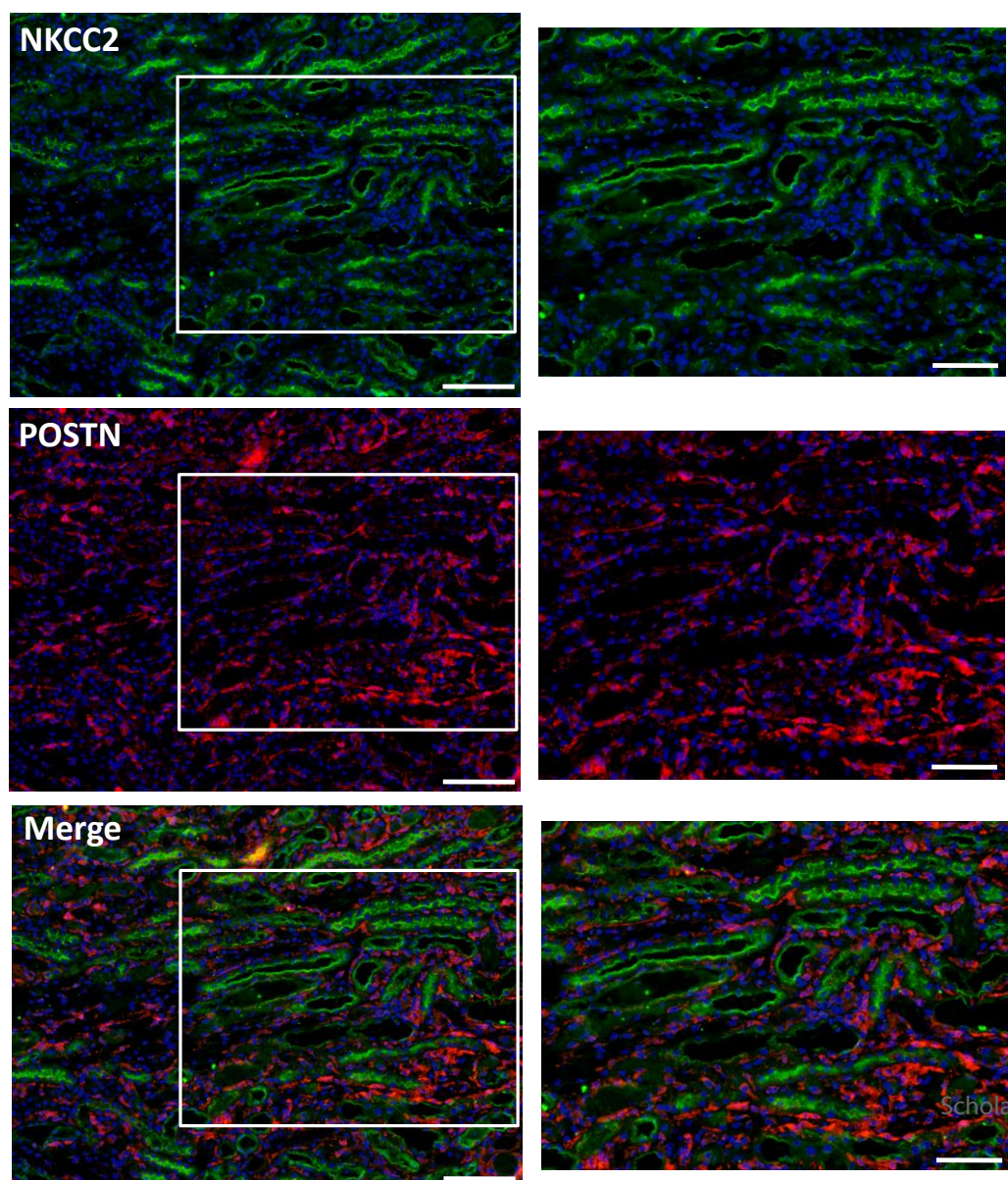
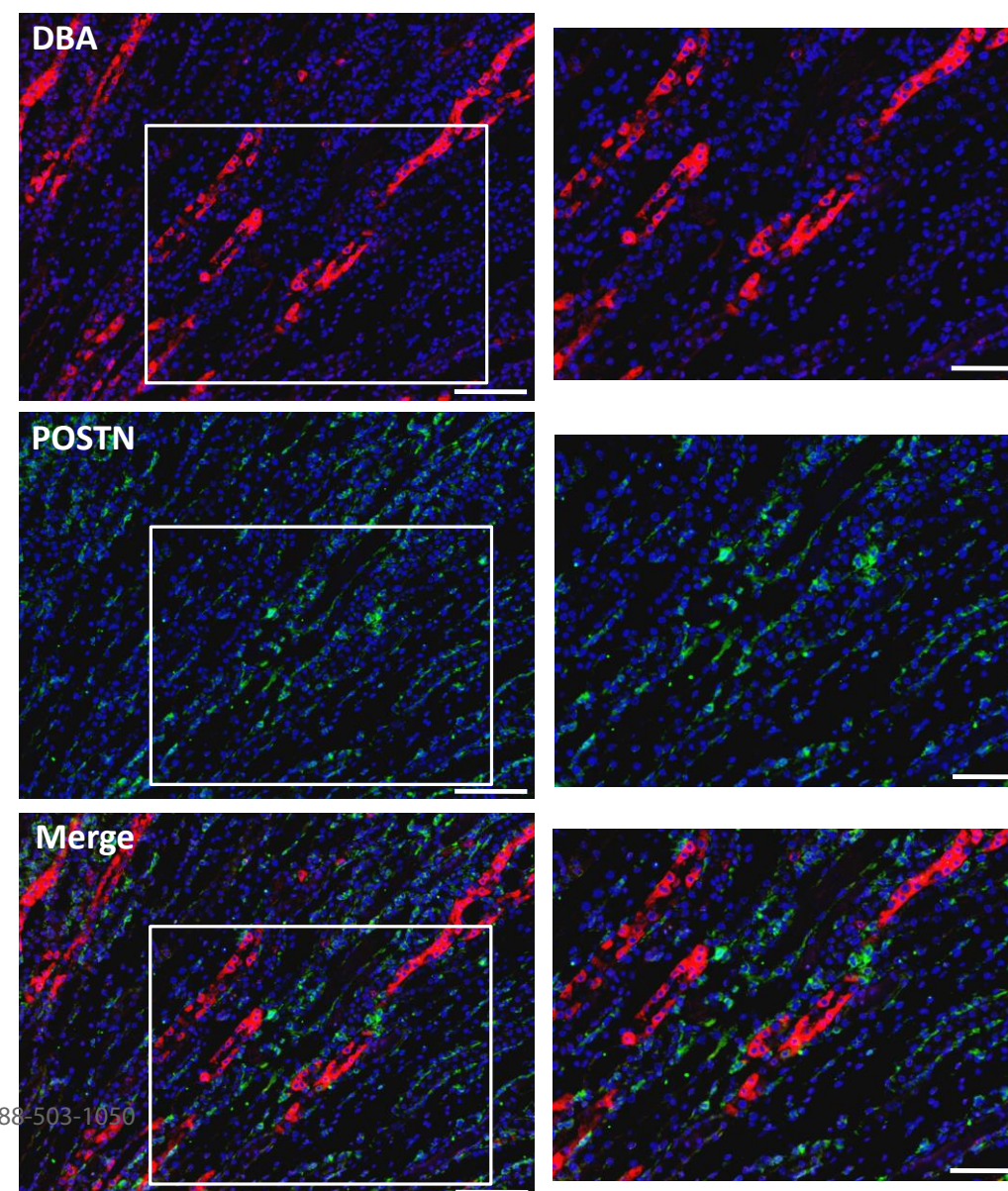


# Figure 7

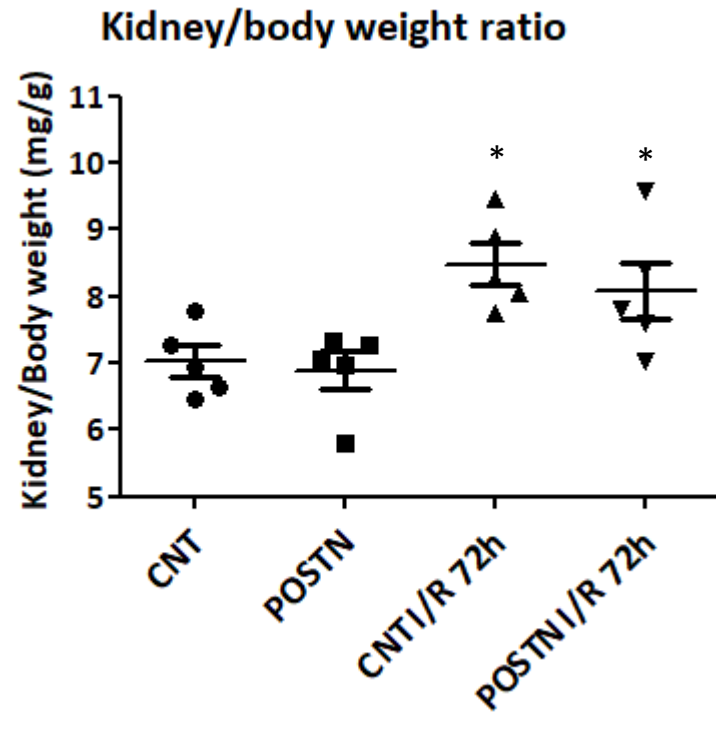


## Figure 8

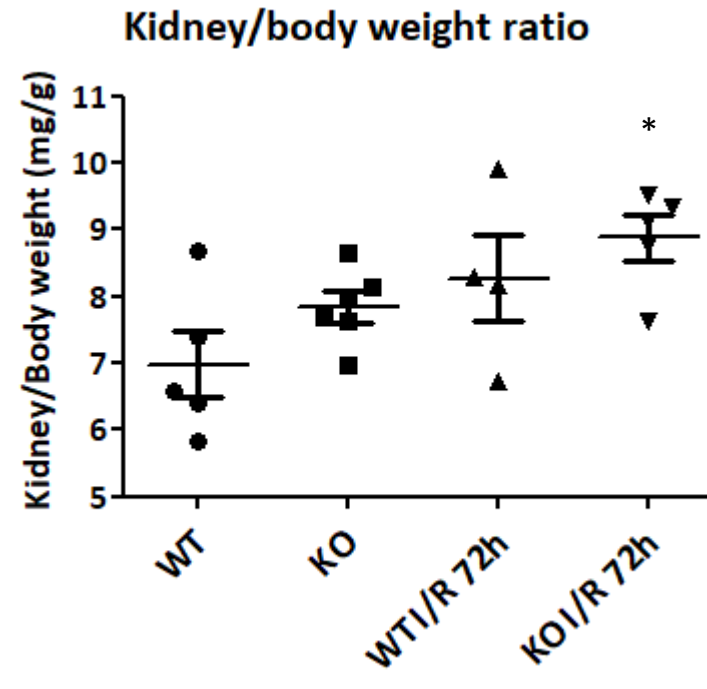


**A****B****C****D**

**A**

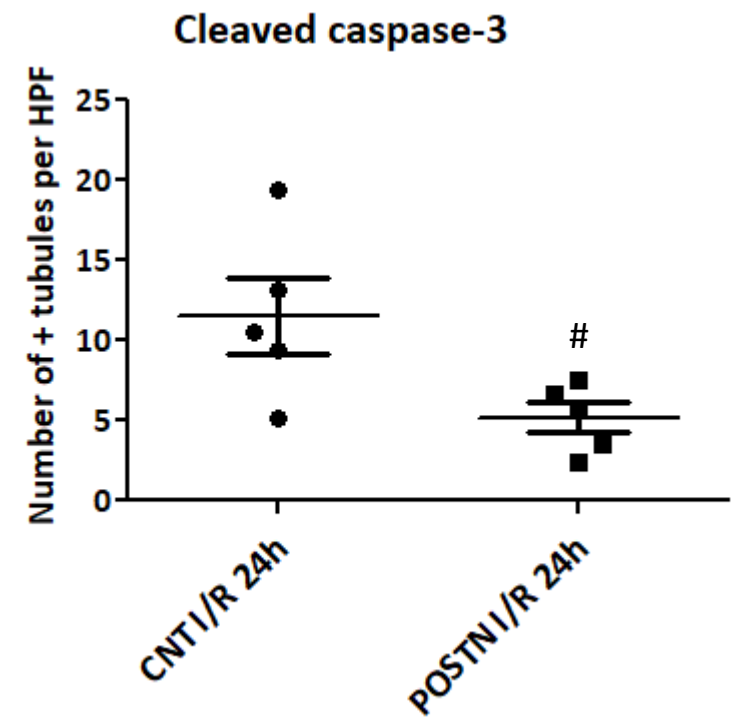
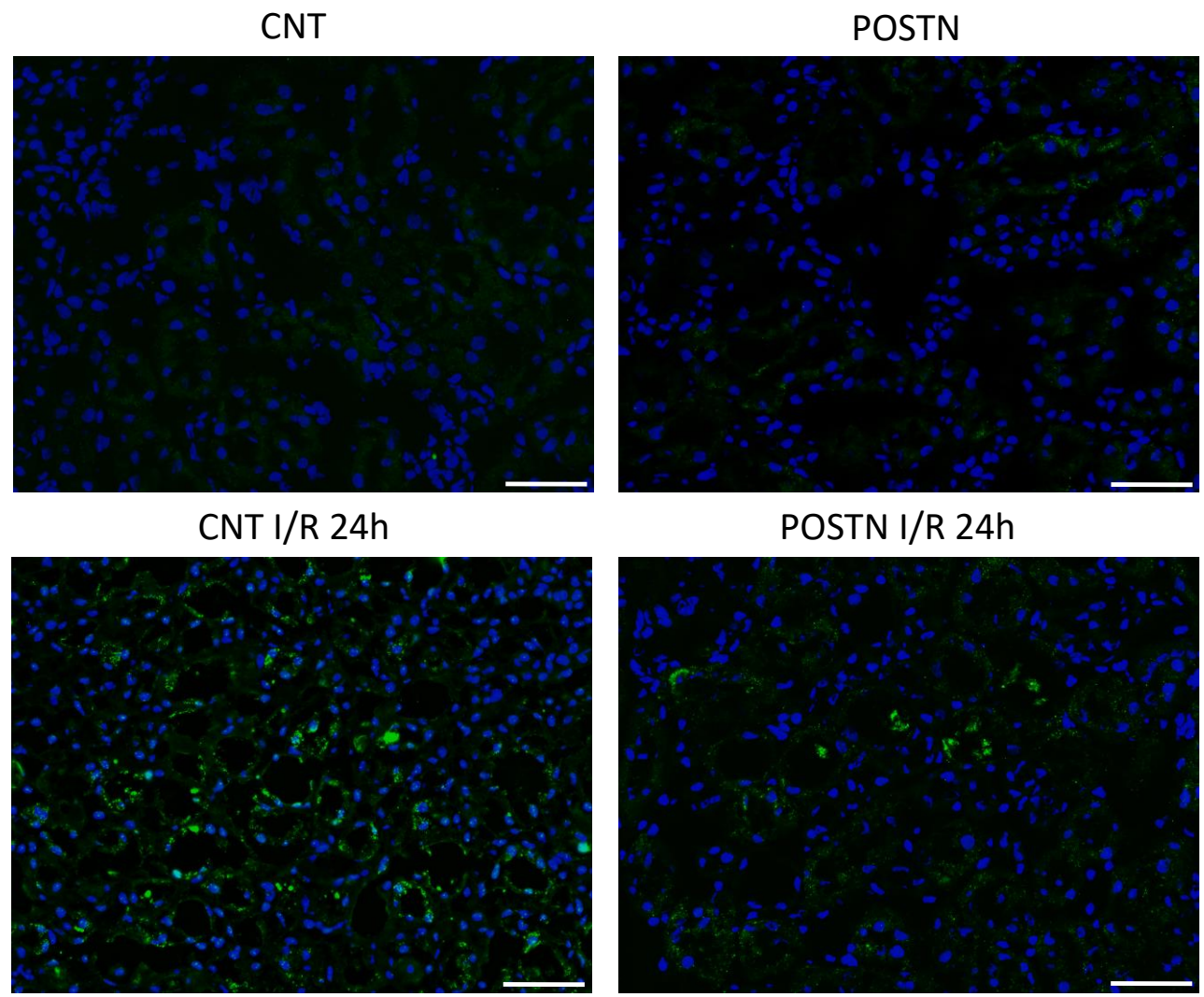


**B**

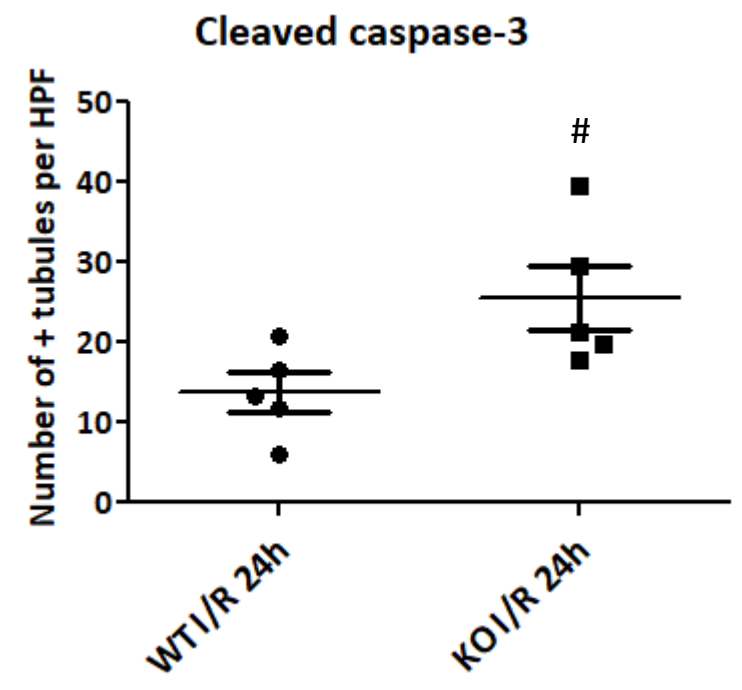
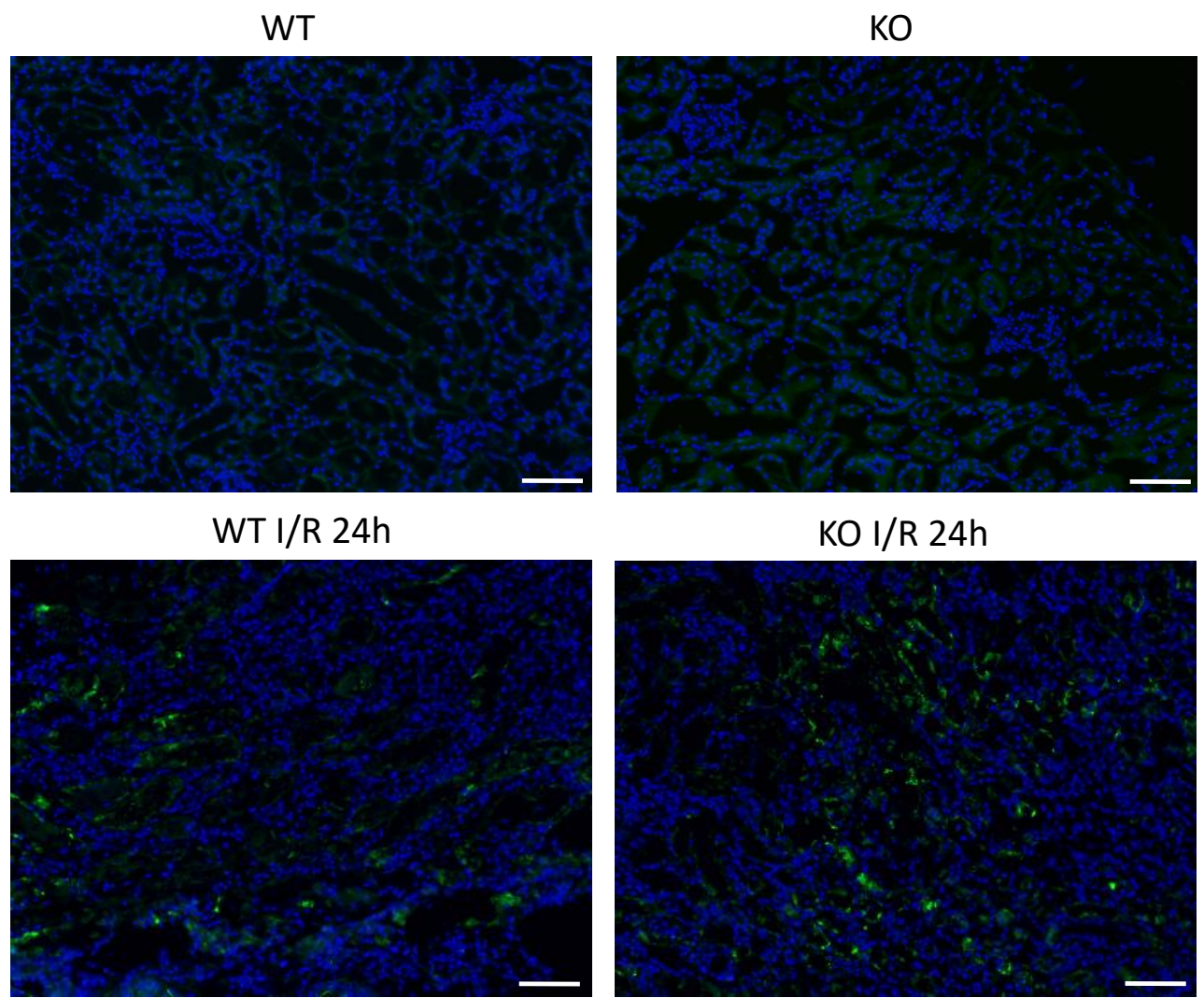


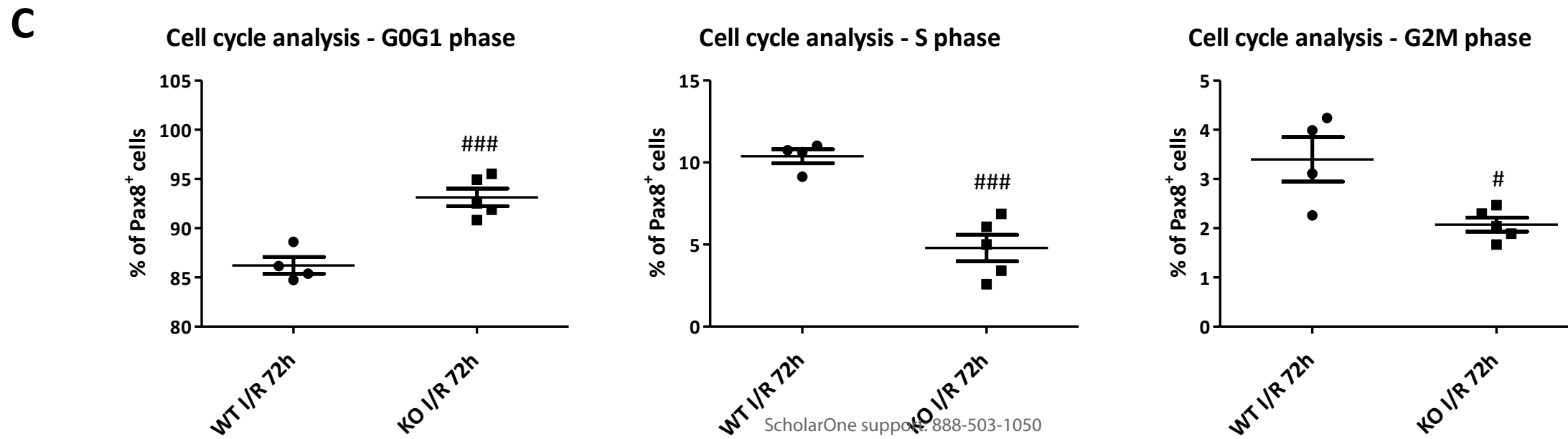
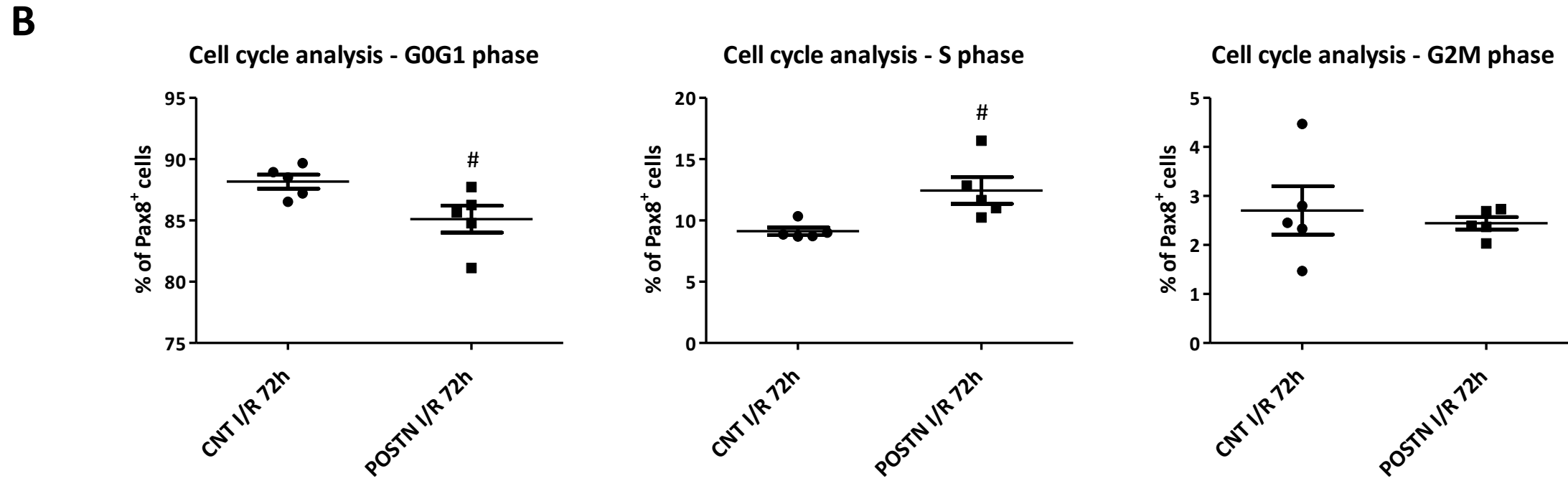
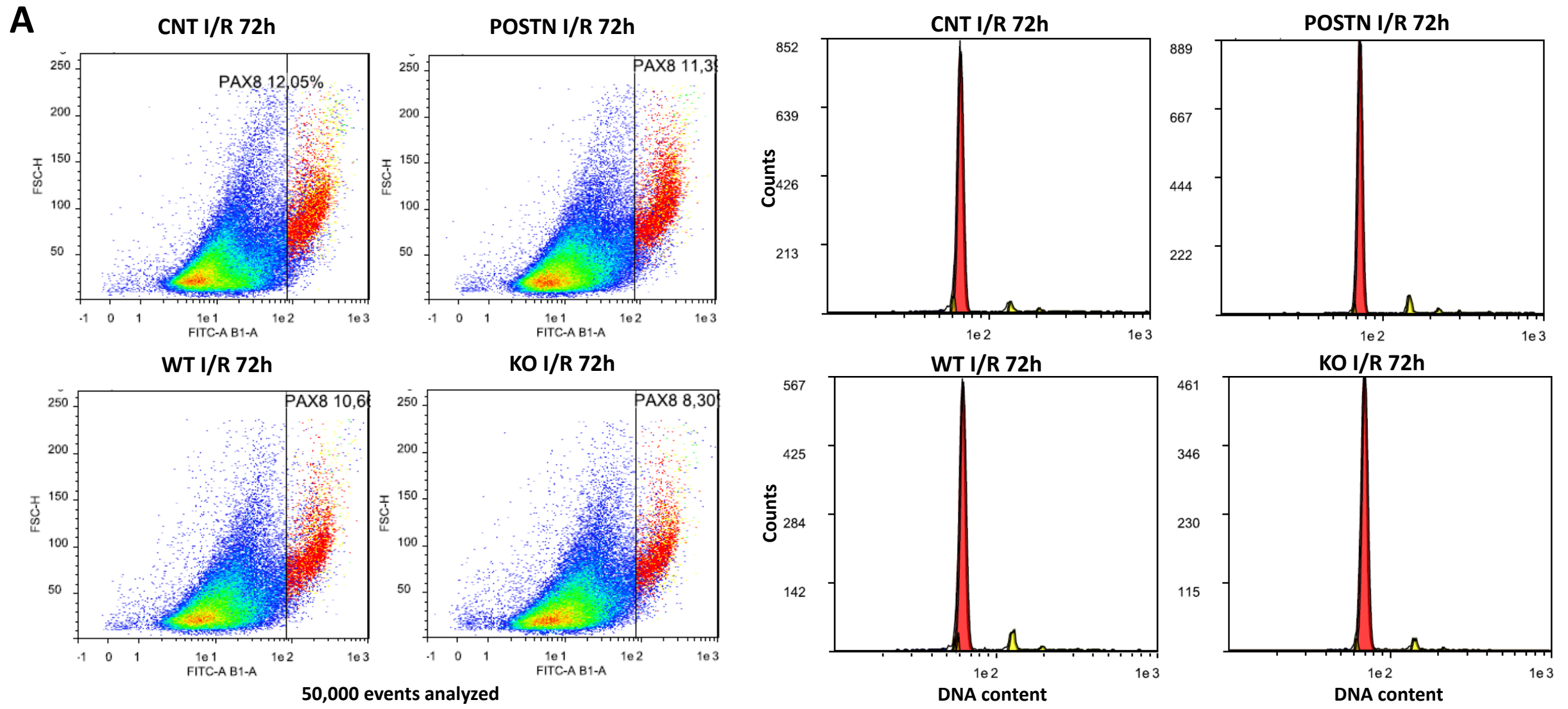
1  
2  
3  
4  
5  
6  
7  
8  
9  
10  
11  
12  
13  
14  
15  
16  
17  
18  
19  
20  
21  
22  
23  
24  
25  
26  
27  
28  
29  
30  
31  
32  
33  
34  
35  
36  
37  
38  
39  
40  
41  
42  
43  
44  
45  
46  
47  
48  
49  
50  
51  
52  
53  
54  
55  
56  
57  
58  
59  
60

**A**

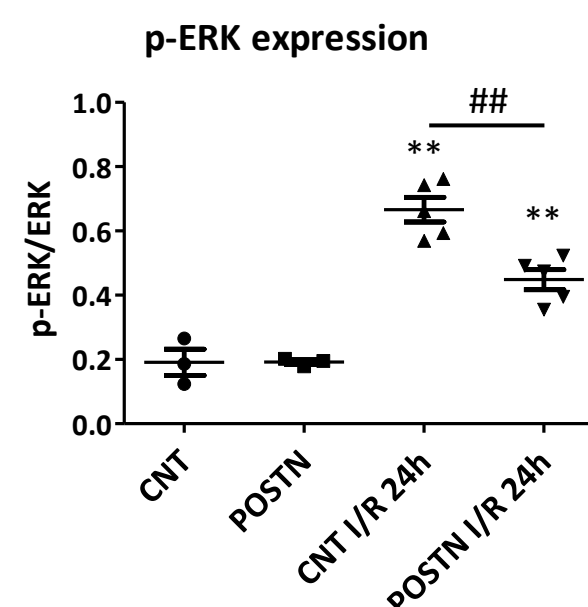
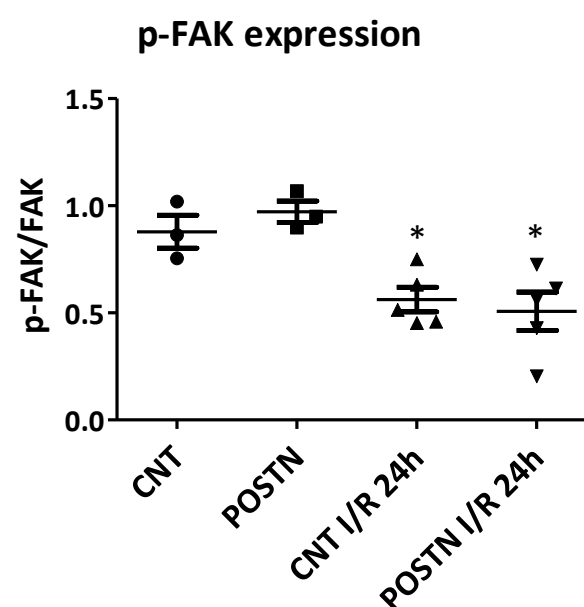
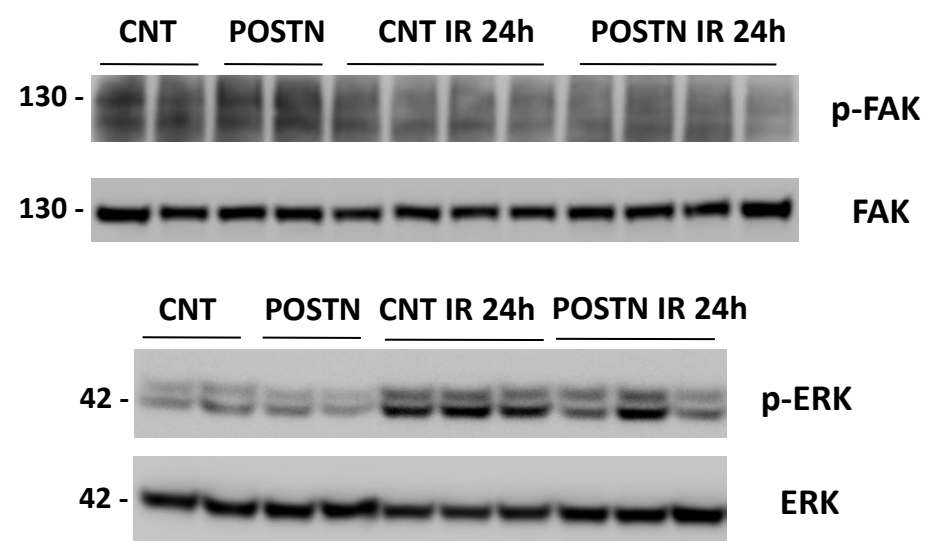


**B**

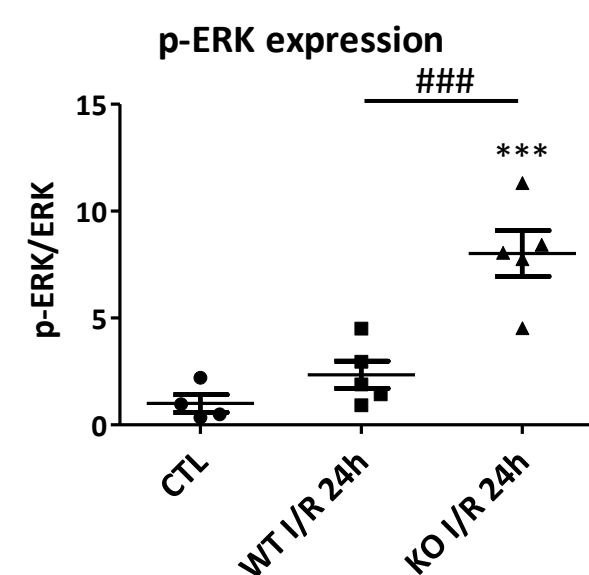
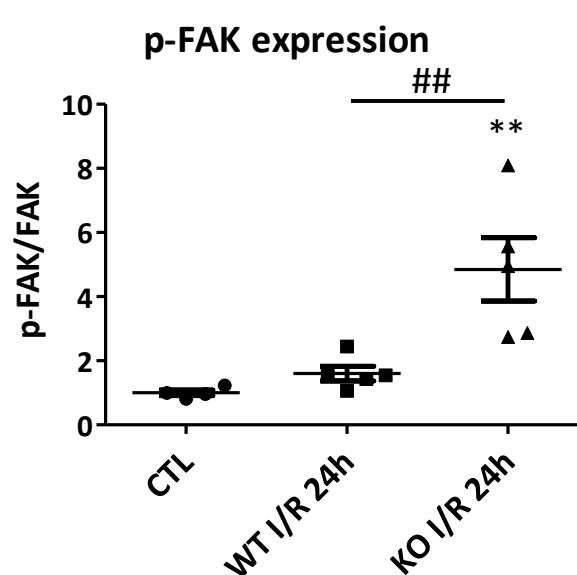
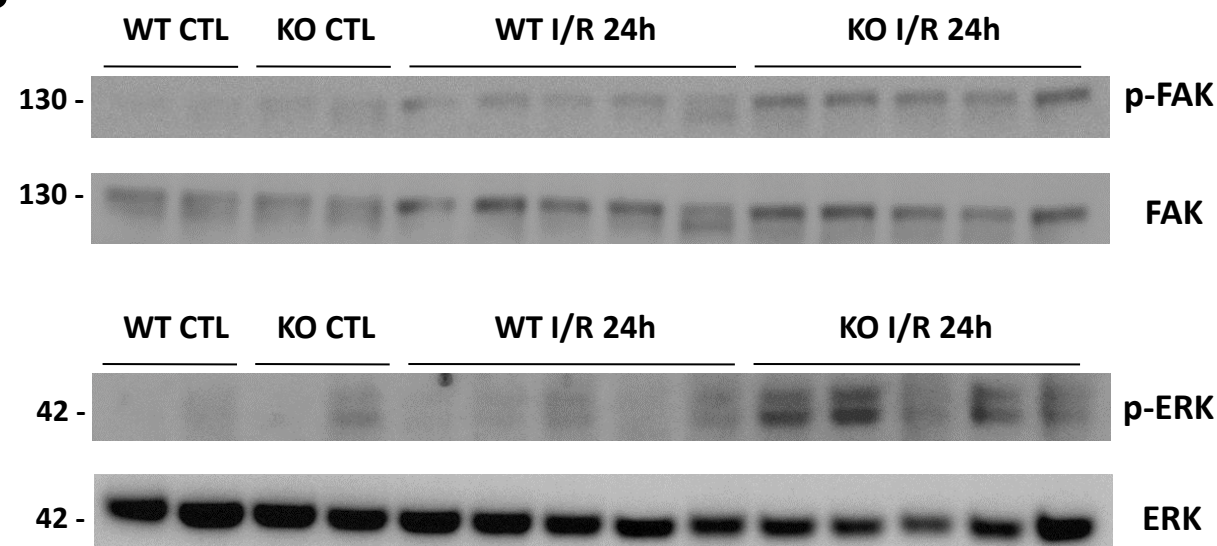


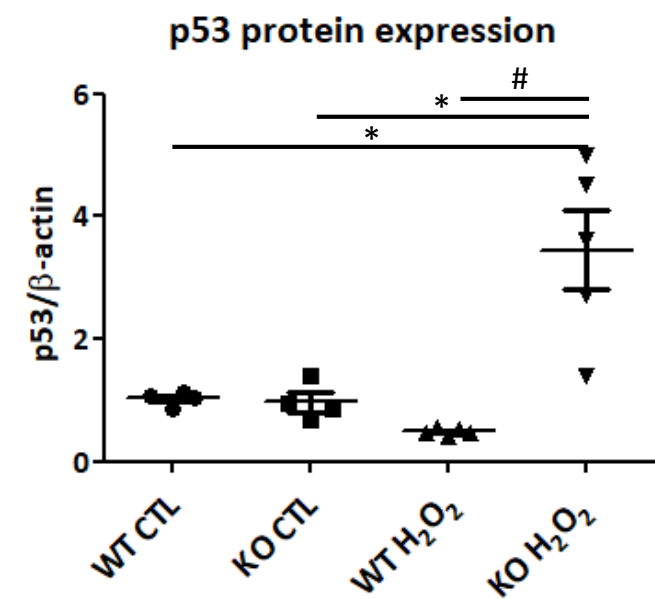
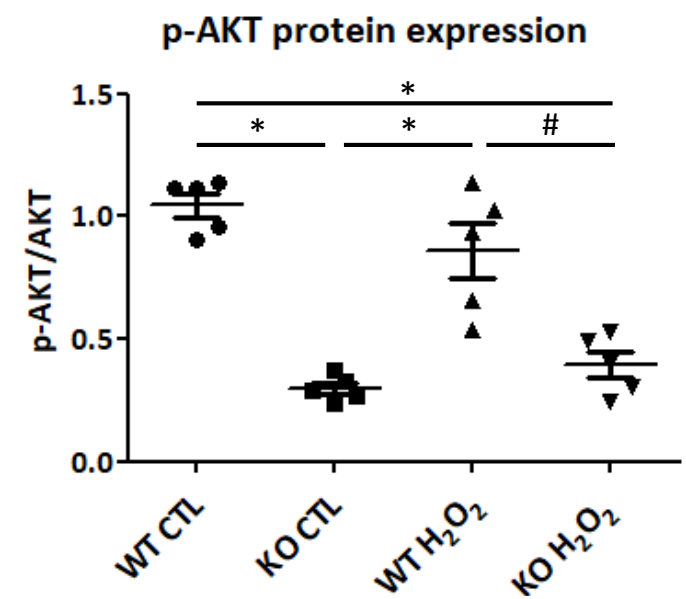
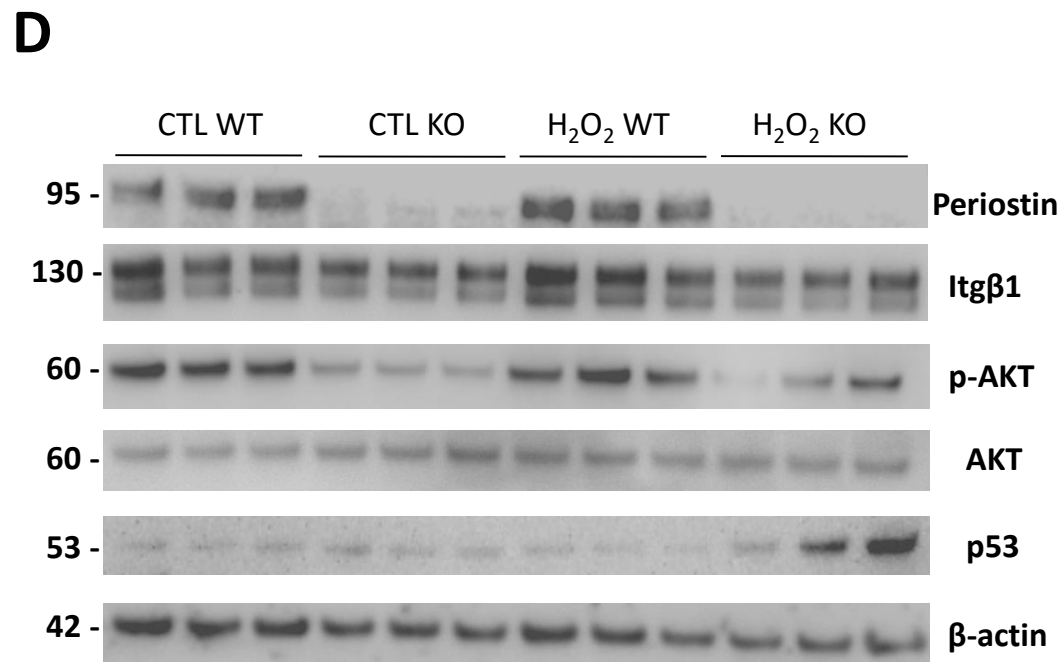
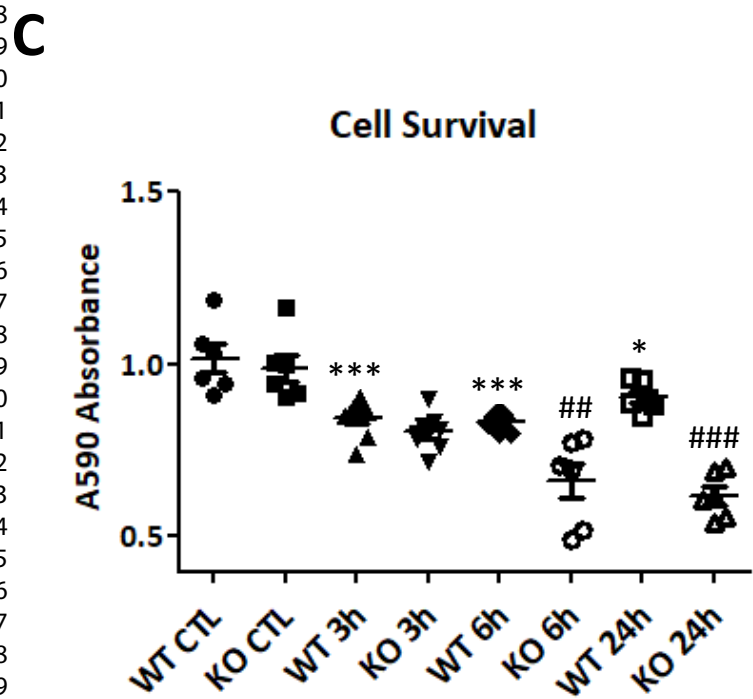
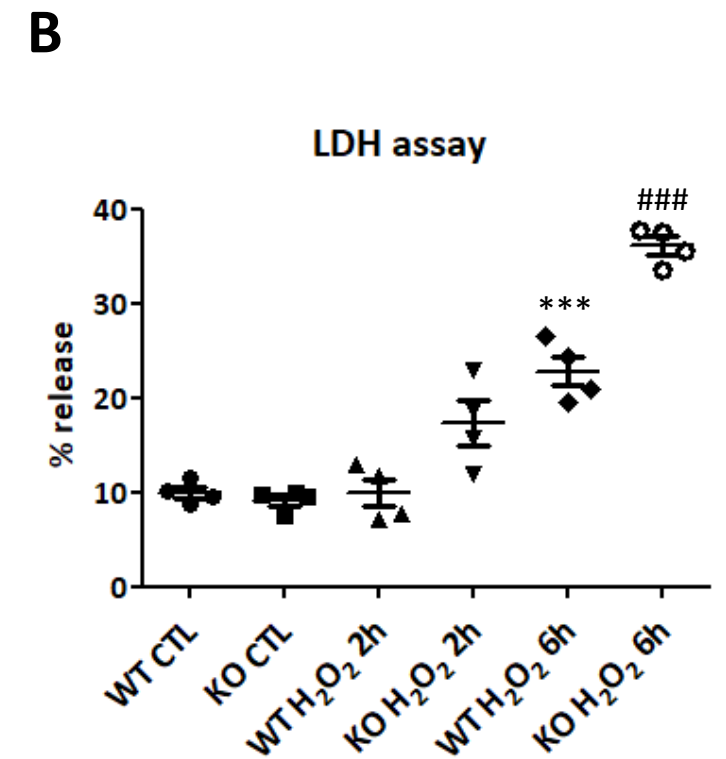
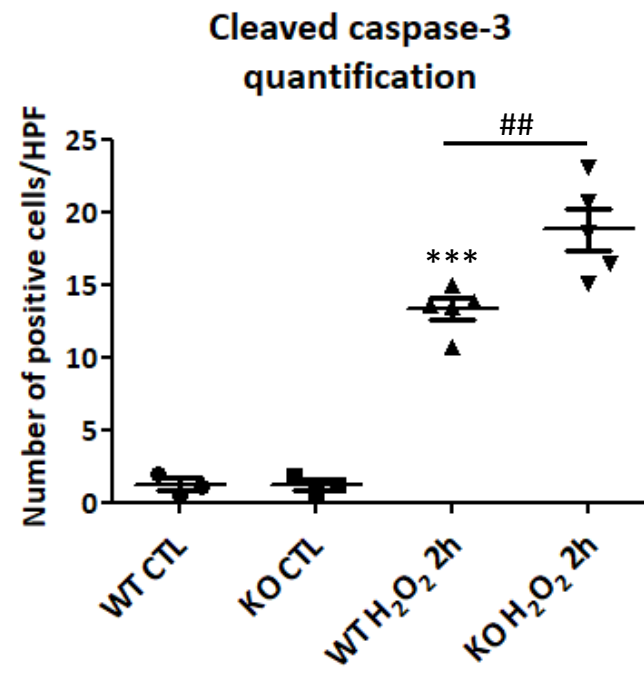
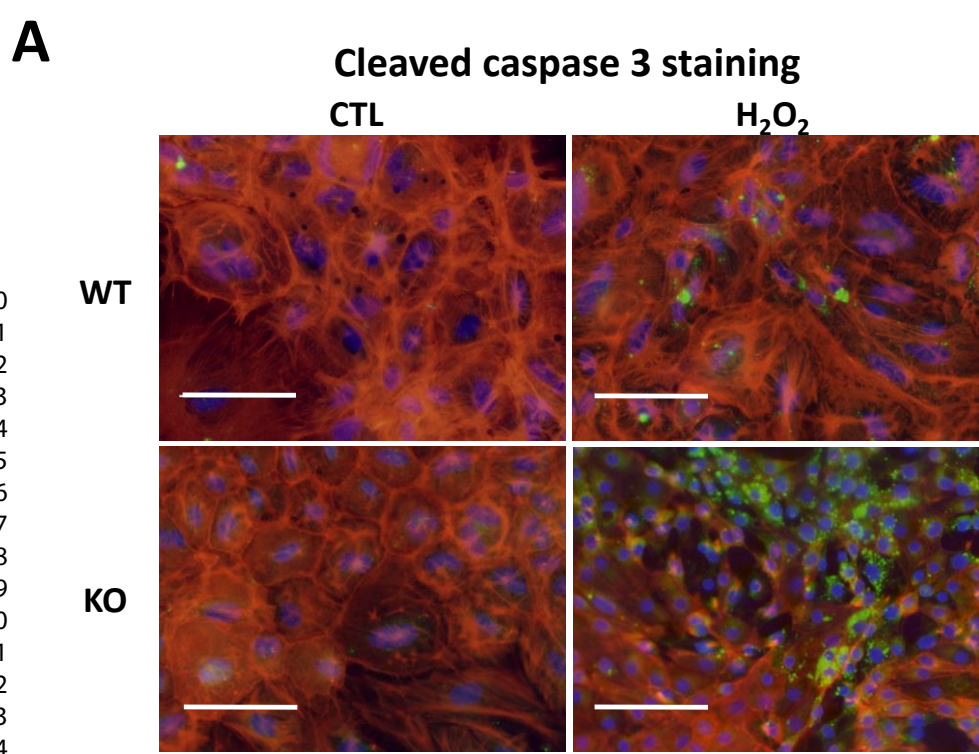


**A**

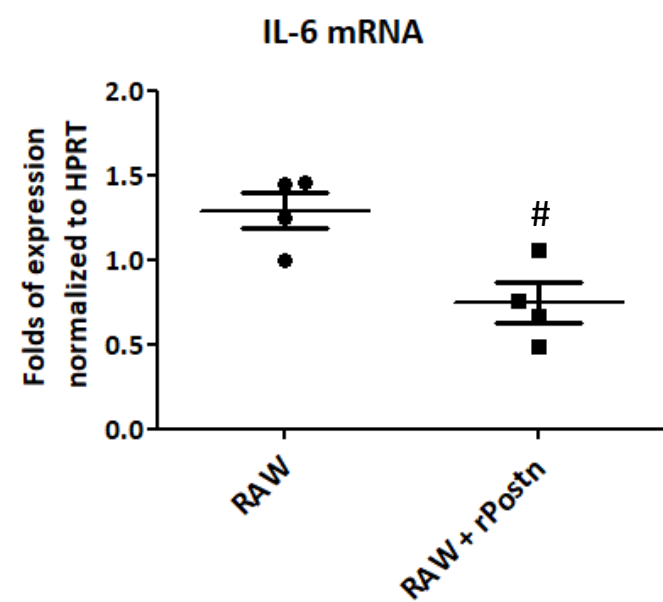


**B**

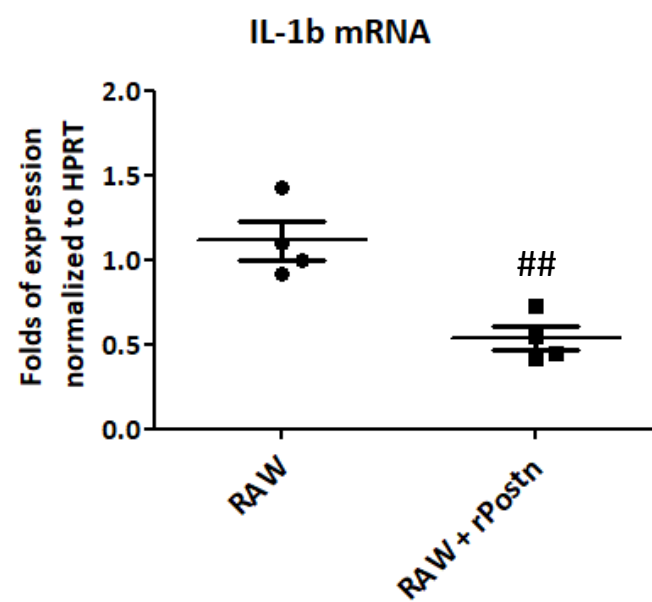




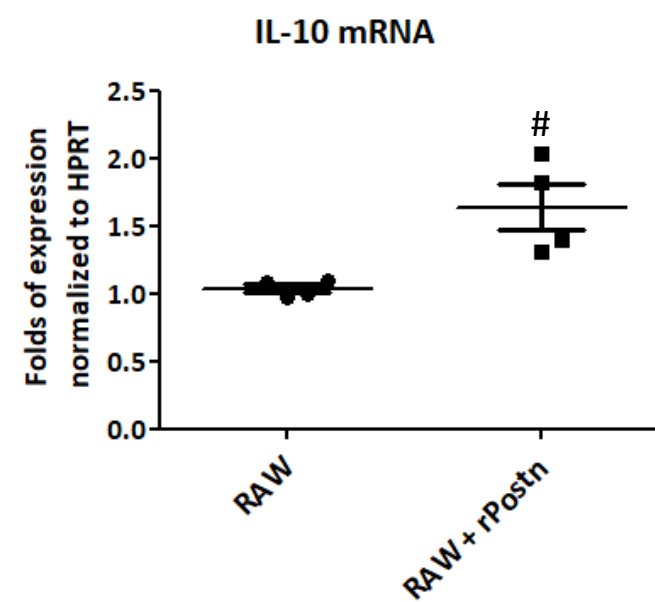
**A**



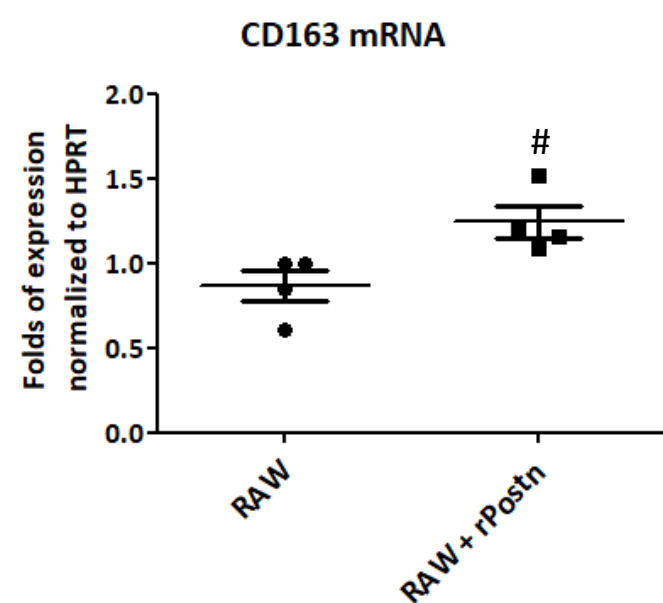
**B**



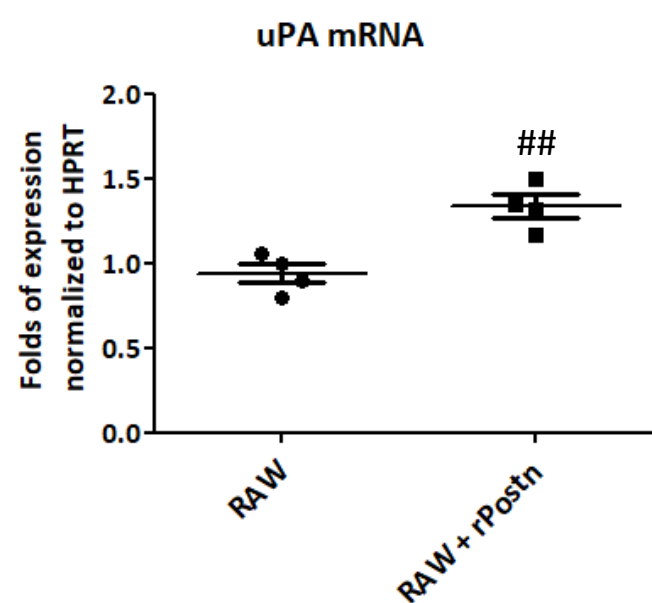
**C**



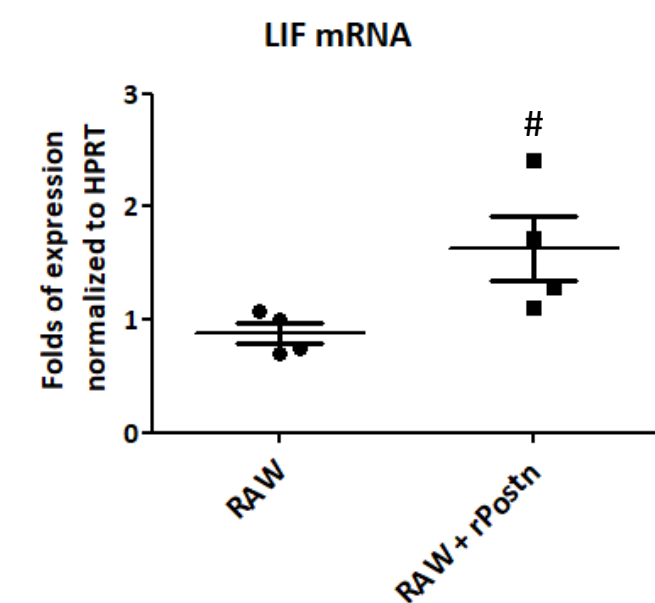
**D**



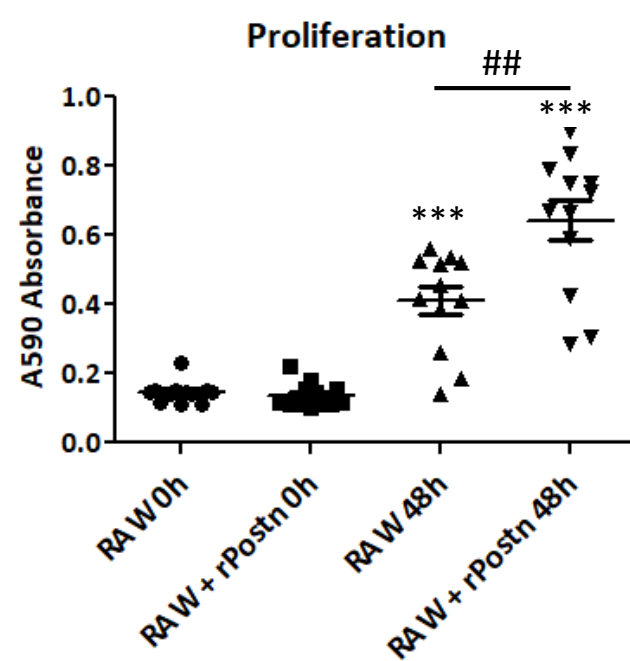
**E**

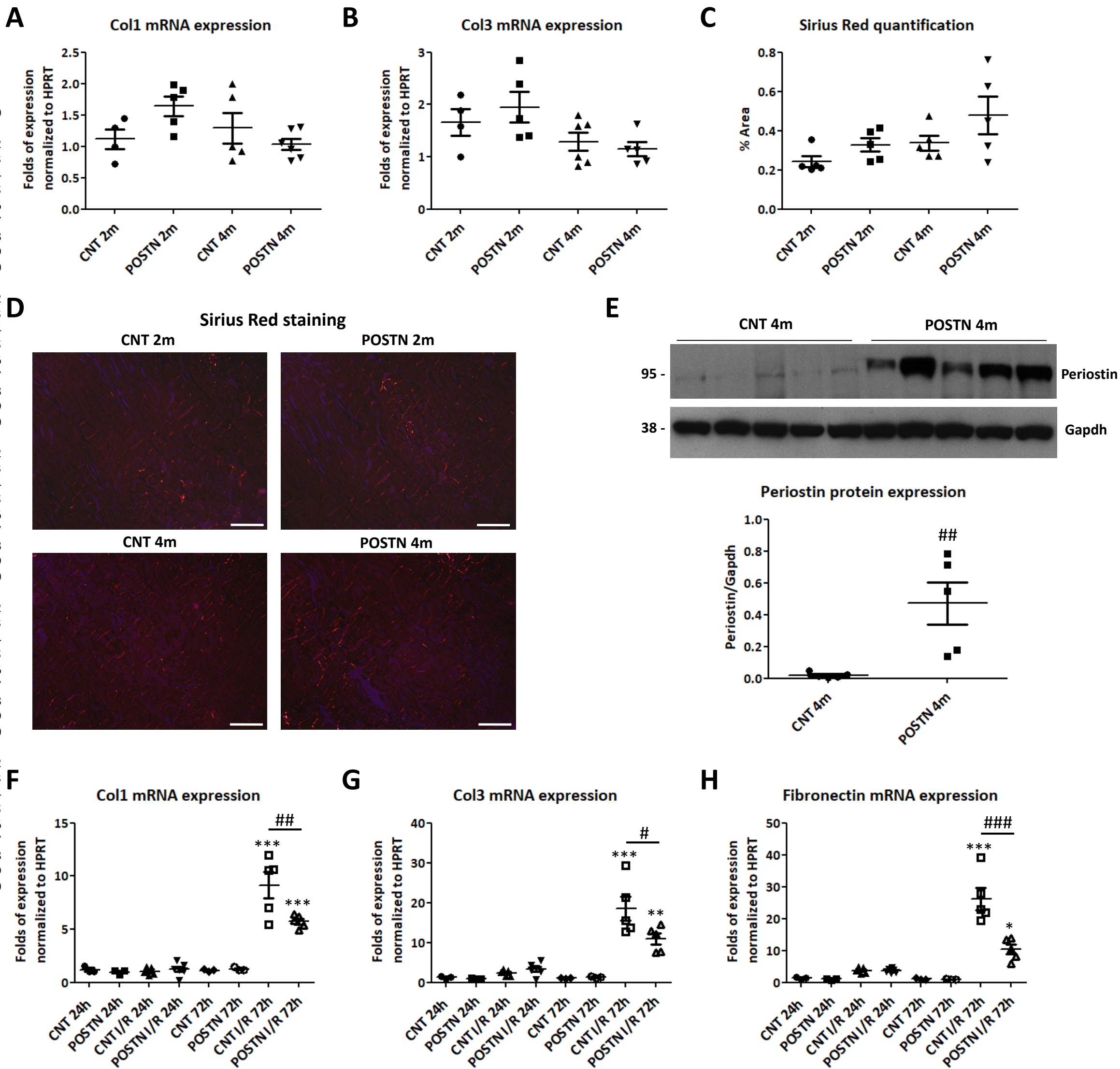


**F**

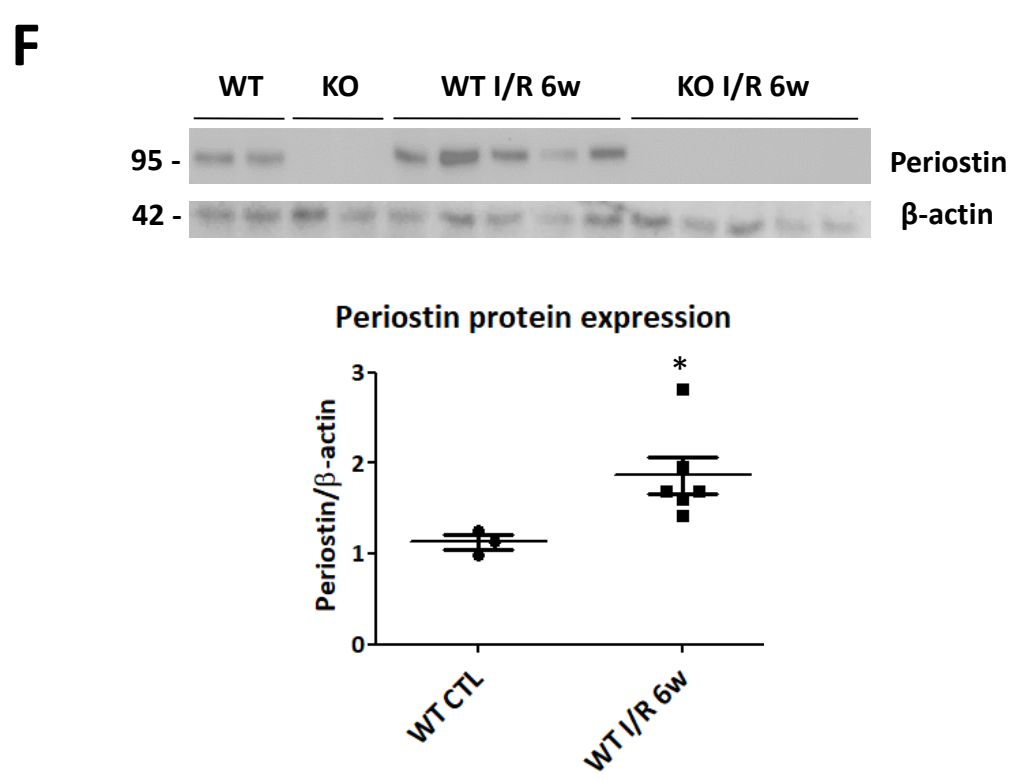
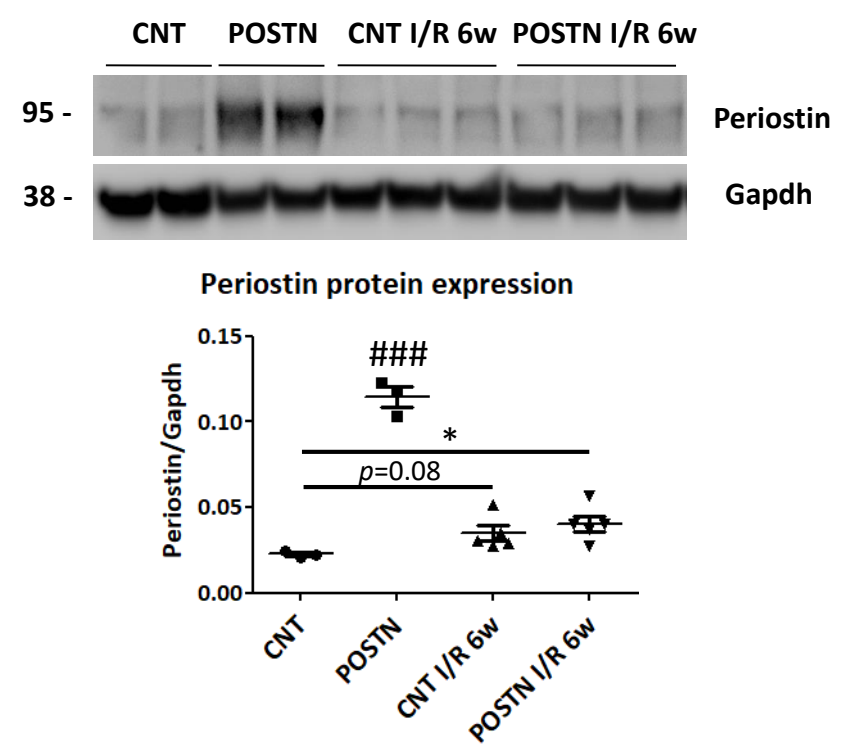
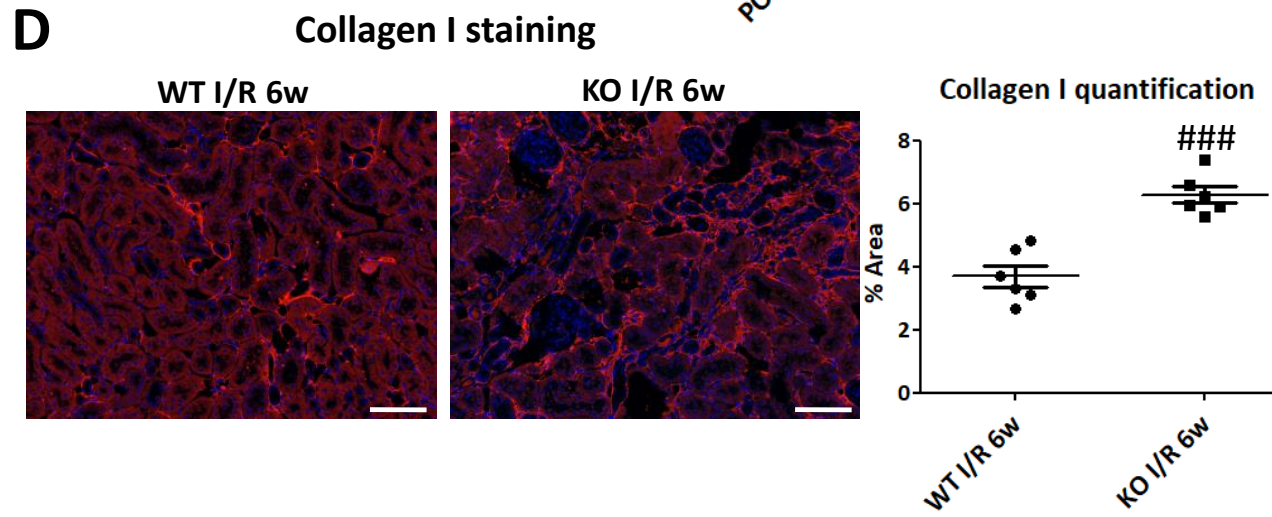
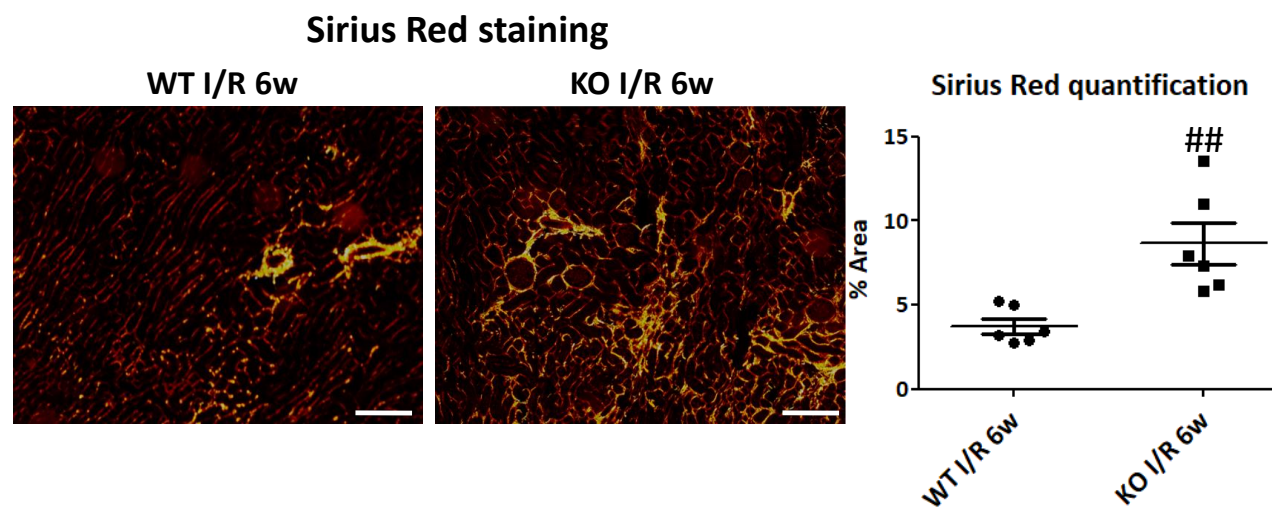
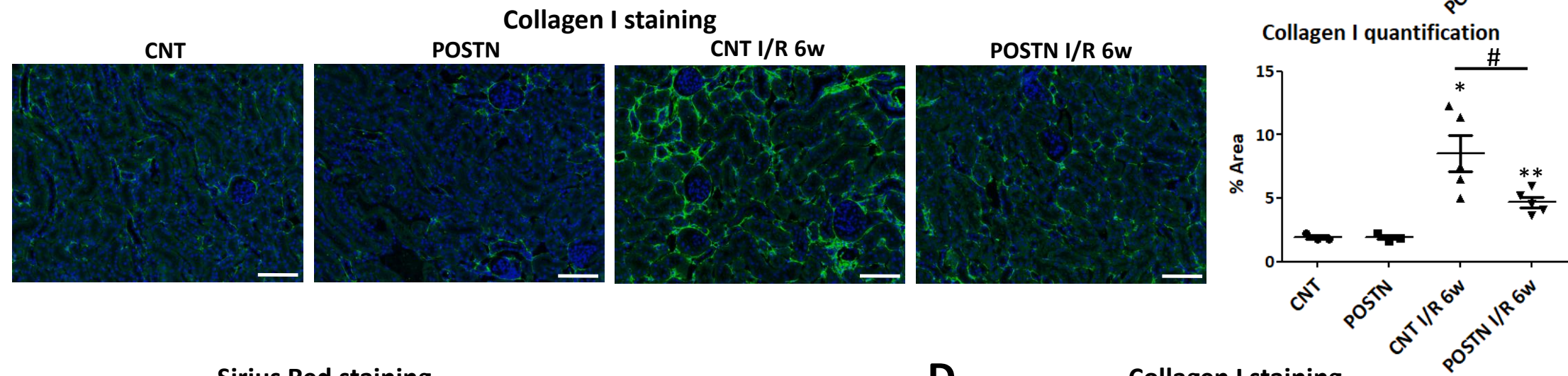
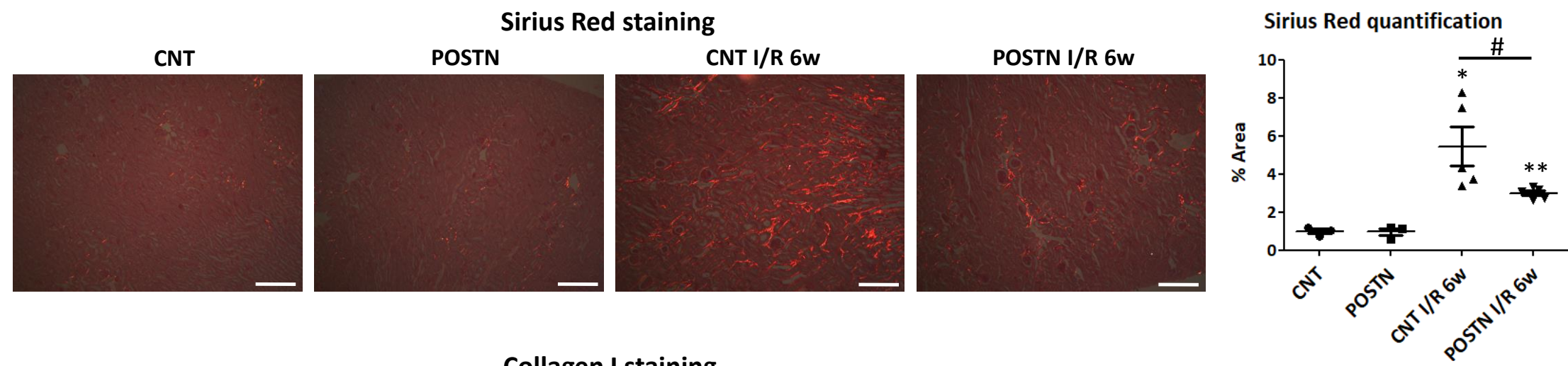


**G**

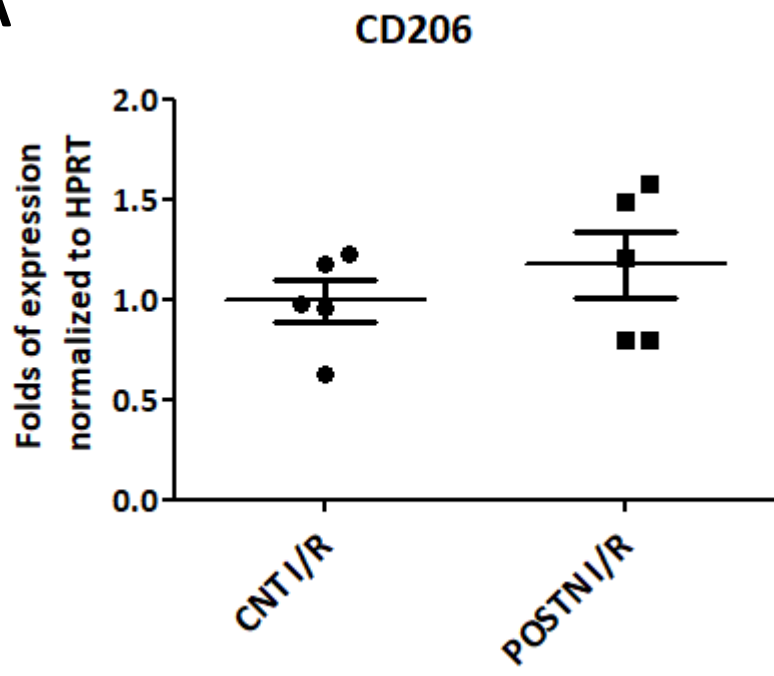




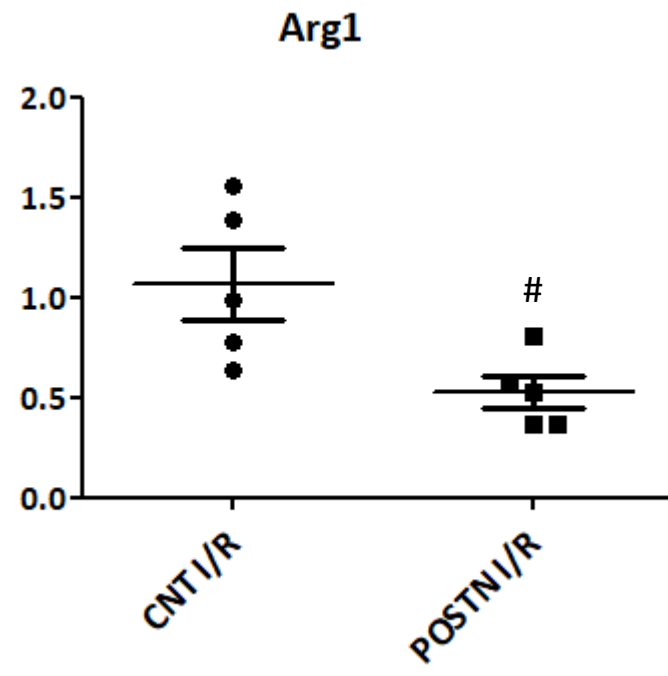
1  
2  
3  
4  
5  
6  
7  
8  
9  
10  
11  
12  
13  
14  
15  
16  
17  
18  
19  
20  
21  
22  
23  
24  
25  
26  
27  
28  
29  
30  
31  
32  
33  
34  
35  
36  
37  
38  
39  
40  
41  
42  
43  
44  
45  
46  
47  
48  
49  
50  
51  
52  
53  
54  
55  
56  
57  
58  
59  
60



**A**



**B**



**C**

